An investigation in the influence of void's shape, distribution and size to the response of pipes during impact

A dissertation submitted to the University of Manchester for the degree of Master of Composite Materials by Research in the Faculty of Science and Engineering

2019

Orestis K. Triantopoulos

Department of Materials

Blank Page

Contents

1. Literature Review 11
1.1 Composites 11
1.2 Composites in offshore structures 12
1.3 Defects/voids 14
1.4 How the voids influence the properties of the structure 14
1.5 Methods for detecting defects(surface/internal) 15
1.6 Impact testing in Composite materials 19
1.6.1 Low velocity impact devices 19
1.6.2 Influence of constituent properties on the impact response of composite materials 20
2 Introduction to the Experimental Methods 21
3 Impact testing 24
3.1 Summary of Impact testing 24
3.2 Method 25
3.3 Errors and Interferences 30
3.4 Conditioning and Test specimens 31
3.5 Impact Tests 31
3.4 Conclusions 35
4. Ultrasonic C-Scan 36
4.1 Method 36
4.2 Results 38
4.3 Conclusions 41
5 Calculation of Void Content through Burn Off Resin Tests 42
5.1 Summary of Burn off Resin Tests 42
5.2 Method – Burn off Resin Test 42
5.3 Errors and Interferences 43
5.4 Conditioning and Test conditions 44

5.5 Test Methods - Measuring Density 45
5.5.1 Method A - Measuring the Density 45
5.6 Burn off Tests 50
5.6.1 Optimal burn off time 52
5.7 Validation of the Void Content Measurement Method 53
5.8 Void Content Measurement 56
6 Inspection of the Damaged Area 57
6.1 Camera 58
6.2 Advanced Camera 59
6.3 Conclusions 61
7 Finite Element Analysis 63
8. Conclusions 74
8.1 Future research 75
8 References 76
8.1 Standards 77

Total Number of Words: 13.005

List of Figures:

Figure 1: Fiber reinforced composite as designed in Abaqus 11
Figure 2: Shear failure modes 12
Figure 3: Composite pipes made by Wavistrong 13
Figure 4: Summary of non-destructive methods 19
Figure 5: Variation of Charpy impact energy with normalised strain energy capacity of fibres [10] 20
Figure 6: Mechanical Properties of the pipe 22
Figure 7: Pipes that were used in the experiments 22
Figure 8: Diamond cutter 23
Figure 9: Rigid Base 25
Figure 10: Flat and curved specimens placed on the plate of the impact machine (the dimensions of the specimen and the fasteners are not proportional) 26
Figure 11: Impact support fixture (Source: ASTM D7136) 26
Figure 12: Mechanical Design of the Custom Fixture made on Solidworks 28
Figure 13: (Left) 3/4'' Twist Drill, (Right) 1-5/8 Twist Drill 29
Figure 14: Completed Custom Fixture 30
Figure 15: (on the left) initial impact tower, (on the right) impact tower used for the tests 32
Figure 16: Fixture fastened on the rigid base 33
Figure 17: Specimen fastened on the fixture 34
Figure 18: Time-Force during the impact event 35
Figure 19: C-scan machine used for the experiments 36
Figure 20: The specimens fastened on the C-scanner 37
Figure 21: Settings of the C-Scan 38
Figure 22: Different areas of the scan 38
Figure 23: 10J Impact energy, 1MHz, High void content on the left and low on the right 39
Figure 24: 20J Impact energy, 1MHz, High void content on the left and low on the right 40
Figure 25: 10J Impact energy, 0.5MHz, High void content on the left and low on the right 40
Figure 26: 20J Impact energy, 0.5 MHz, High void content on the left and low on the right 41
Figure 27: The extracted specimens from a damaged laminate 46
Figure 28: Void content of the 4 corners of the impacted specimen 46
Figure 29: Balance 47
Figure 30: Standard Density of Water 49
Figure 31: Laser thermometer 51
Figure 32: Specimen after resin- burn off test 52

Figure 33: Burned specimens (6000C) of the parametric study used to identify the optimal burn time 53
Figure 34: Measured weights 53
Figure 35: Theoretical Density 55
Figure 36: Calculated void content 56
Figure 37: Void content of the impacted specimens 56
Figure 38: Impacted specimen cut in the middle with a diamond cutter 57
Figure 39: Grinding sheets (P400, P600, P800, P1200, P2400, P4000) 58
Figure 40: Photo of the impacted area using a regular camera 59
Figure 41: Photo of the impacted area using the advanced camera 60
Figure 42: Close up photo of the impacted area using the advanced camera 61
Figure 43: Illustration of the impactor and the laminate 64
Figure 44: Continuum shell vs conventional shell elements (Source: 6.14 Abaqus Documentation) 65
Figure 45: Filament winding (Source: i.ytimg.com) 66
Figure 46: Interaction between the impactor and the laminate 66
Figure 47: Boundary conditions 67
Figure 48: Amplitude / Time- Displacement 68
Figure 49 Stress distribution of the upper face based on Von Mises failure criterion 70
Figure 50: Stress distribution of the bottom face based on Von Mises criterion 70
Figure 51: Stress distribution in the Y-axis 71
Figure 52: Displacement distribution in the Y-axis 72
Figure 53: Illustration of the deformed laminate 73

Abstract

During the last two decades composite materials have been proved to be the most suitable solution for lightweight structures, mainly in Aerospace Industry. In offshore structures, pipes that are made from metals have approached the limit of their performance and due to corrosion resistance, low density and longer life-time the use of composite materials in Gas and Oil Industry has been grown, as well.

This study is focused on the way that the presence of voids influences the impact response of pipes made with glass fibre reinforced polymer composites. In this study, the whole pipe is replaced with a curved section in order to reduce the time and complexity of the experimental set up and numerical simulation. Initially, ultrasonic C-Scanning will give a generic and qualitive image of the amount, the shape and distribution of the voids introduced during pipe fabrication. The specimens will then be exposed to low-velocity impact with the aim to examine how the void geometric parameters influence their mechanical behavior. Quantitative results regarding the exact void content will be extracted via resin burn-off tests. These tests will be carried out after impacts, since the former constitutes a destructive testing method. The specimens will be C-scanned to observe how impact induced damage interacts with void content. A better understanding of the process will lead to improved fabrication method, revision of pipe test standards and increased fatigue life of the pipe.

Declaration

DECLARATION

No portion of the work referred to in the dissertation has been submitted in support of an application for another degree or qualification of this or any other university or other institute of learning.

COPYRIGHT STATEMENT

i. The author of this dissertation (including any appendices and/or schedules to this dissertation) owns certain copyright or related rights in it (the “Copyright”) and he has given The University of Manchester certain rights to use such Copyright, including for administrative purposes. ii. Copies of this dissertation, either in full or in extracts and whether in hard or electronic copy, may be made only in accordance with the Copyright, Designs and Patents Act 1988 (as amended) and regulations issued under it or, where appropriate, in accordance with licensing agreements which the University has from time to time. This page must form part of any such copies made. iii. The ownership of certain Copyright, patents, designs, trademarks and other intellectual property (the “Intellectual Property”) and any reproductions of copyright works in the dissertation, for example graphs and tables (“Reproductions”), which may be described in this dissertation, may not be owned by the author and may be owned by third parties. Such Intellectual Property and Reproductions cannot and must not be made available for use without the prior written permission of the owner(s) of the relevant Intellectual Property and/or Reproductions. iv. Further information on the conditions under which disclosure, publication and commercialisation of this dissertation, the Copyright and any Intellectual Property and/or Reproductions described in it may take place is available in the University IP Policy, in any relevant Dissertation restriction declarations deposited in the University Library, The University Library’s regulations and in The University’s policy on Presentation of Dissertations

Acknowledgement

The author would like to thank Prof. C. Soutis (University of Manchester) and Dr. W. Harris (University of Manchester) for their constructive criticism and supervision.

I would also like to thank Mrs. Magdalini Papanaoum for her collaboration during this project.

Introduction

This research was conducted trying to follow the standards and other research that was made in this area. However, there was very limited literature for curved composite laminates made of glass fibres. For this reason, the literature for flat composite laminates made of glass fibres was used as a guiding point. As the research was progressing, less and less literature was available, and more initiative was introduced. Some new methods and techniques were invented with the hope that they could help other researchers to progress this area of composite materials.

1. Literature Review

This study is focused on how the existence of voids influences the impact response of pipes made with composite materials. For the purposes of this study impact testing, visual inspection, C-scanning, resin- burn off tests, diamond cutting and finite element analysis will be carried out. Initially, it is important to review a few papers for a better understanding of the nature of the composite mechanics, their failure mechanisms and similar studies that may have been conducted.

1.1 Composites

A composite material is made of at least two constituents in a macroscopic scale, the matrix and the reinforcements. This research will be focused on the fibre reinforced polymers (FPR). FPRs consist of fibre reinforcement and a polymer matrix which can be either a thermoset or a thermoplastic.

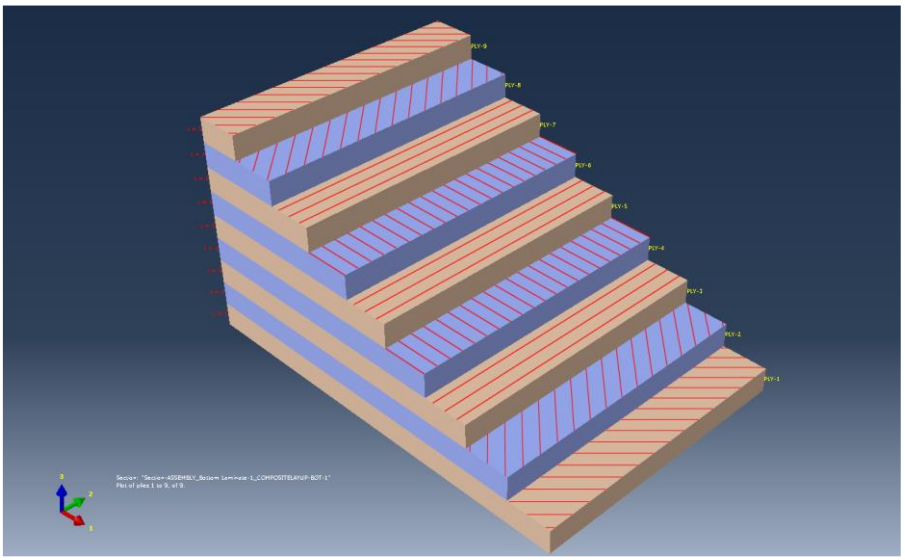

Figure 1: Fiber reinforced composite as designed in Abaqus

There is a number of different failure modes that can occur in a structure that is made of composite materials:

i) Matrix failure in tension
ii) Fibres failure in tension
iii) Matrix failure in compression
iv) Fibres failure in compression
v) Shear failure or delamination

Shear failure occurs between the plies and is due to shear stresses in the interface between the layers. There are two different shear failure modes as shown in the picture below. The failure mode that will occur each time depends from the fracture energy, which is the minimum energy that is required for any of the (see picture below) failure modes to take place. A combination of the mode I and mode II is called mixed-mode.(Charalambides, Kinloch, Wang, & Williams, 1992)

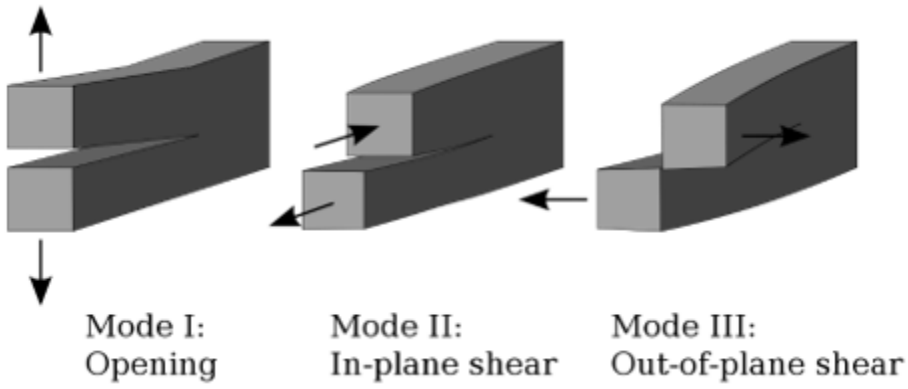

Figure 2: Shear failure modes

A combination of the mode I and mode II is called mixed-mode.

1.2 Composites in offshore structures

Approximately 200 billion barrels of oil reside in undiscovered deepwater (Ozden O. Ochoa, 2005). The quest to getting access those reserves has already started and composites are the most economical leading option. Thus, the use of composite materials in the offshore gas and

oil industry is rapidly expanding. The marine environment requires the use of materials with high stiffness, toughness, resistance to corrosion and long lifetime, so the FPRs (Fibber Reinforced Plastics) are suitable.

Even though there is broad experience with pipes made of steel, their concept is becoming out of place for two main reasons. They cannot go deeper than 1500m and in that depths the total weight of the pipes is extremely heavy and requires high axial tension machines that can be accommodated only by constructing a bigger platform. The introduction of composite pipes can extend the range to more than 3000m while reducing the installation cost up to 37%. (Salama MM, 2001).

There are mainly 4 reasons that are obstacles for this implementation.

- There is limited database for long term damage mechanisms for the prediction of the life expectancy.
- The constructions need to be verified and certified with full scale testing.
- Limited standards and regulations.
- Non-destructive testing and in-site monitoring is required.

This research is studying a very small area of those obstacles that has not yet been studied. The low-velocity impact behaviour of FPRs offshore pipes and how their voids affect this property.

Figure 3: Composite pipes made by Wavistrong

1.3 Defects/voids

Polymer matrix composites can be manufactured with liquid moulding, compression moulding injection moulding, resin fusion compression flow forming and several other techniques. They can be joined with mechanical fastening, adhesive bonding, fusion bonding, etc. (J.-A.E. Manson, 2000) Each manufacturing, processing and joining technique under any circumstance will induce defects in the polymer matrix composites. They can be categorized based on their location. There are fibre, matrix and interface defects. Fibre defects can be broken or misaligned fibres and waviness or irregularities of the fibres in the matrix. Matrix defects can be voids or incomplete curing. Interface defects can be incorrectly bonded regions on fibre surfaces or between the layers. (Hansong Huang, 2005)

Voids are pores that remain unoccupied in a composite material. Voids are usually the result of an imperfection during the processing or manufacturing of the composite material. A void is a non-uniformity of a composite material and it can greatly affect the lifespan and mechanical properties of the composite. (ASTM D2734 – 09) Voids can be found in all the polymer matrix composites (PMC). There are some manufacturing process parameters that can affect the voids content. Such parameters are the cure temperature, the resin viscosity (flow kinematics), the vacuum pressure and the consolidation pressure. Lower resin viscosity and higher cure temperature and vacuum pressure can decrease the voids content significantly.

The composite materials are inhomogeneous so the form of the defects and the way that they affect the mechanical properties are very different and harder to predict than the metallic materials. Generally, in the composite materials the damage does not accumulate in the form of a single flaw, but instead by initiation of a big number of defects in the matrix that can potentially lead to delamination. (Bar-Cohen Y, 1982)

1.4 How the voids influence the properties of the structure

As the void content increases, some material properties (like the flexural modulus, the interlaminar fracture toughness, the fracture toughness energy and the fatigue strength) are expected to drop. (Lin Ye, 1993; P.-O. Hagstrand, 2005) It is worth mentioning, that in some cases fundamental structural flexural properties (like the flexural load at break, the EI and the beam stiffness) will not appear to have their highest values when the void content is zero but in reality, they exhibit their highest values at medium levels of void content. A higher void

content increases the thickness of the structure and even though that translates to lower mechanical properties this could to an overall stronger structure. (James C., 1995)

1.5 Methods for detecting defects(surface/internal)

NDT (Non-Destructive Testing) are the techniques that are used in order to examine a component, material or system without destroying it or affecting its structural integrity and functionality. The basic principal of NDT is to define an object's quality or structural integrity with a non-destructive way via monitoring a natural phenomenon that does not affect the object which is under examination. The inspection using NDT can take place after primary processes (forging, casting, extrusion etc), secondary processes (machining/thermal treatments, welding, platings, etc) and in-service damages (cracking, corrosion, thermal damage, etc.).

The use of NDT has many advantages. The component which is under examination is still functional after the testing. The testing in many occasions can take place during the operation and the equipment is portable. However, the results depend on the inspector. In addition, some methods do not provide a permanent monitoring and cannot detect the orientation of the defects. (Salkind, 1976)

Modern NDT is used extensively in an industrial scale in order to inspect power plants, cables, storage tanks, aircrafts, airplane engines, etc. NDT can:

- ensure the structural integrity and therefore the reliability of the product
- avoid unexpected failure, accidents and protect human life
- increase profit
- contribute to better product design
- examine production processes and reduce costs
- ensure a constant quality level
- guarantee whether the product is ready to use

The inspection range is not always 100%. It depends on the application, the security level that is associated with and the costumer's requirements. When a full inspection range is not possible statistical methods are applied in order to find the fault or defect probability.

A failure of the non-destructing testing to detect crucial defects in safety relevant components can lead to catastrophic consequences for the people and the environment. Thus, all the factors that influence the liability of the NDT methods need to be assessed. The

liability of the NDT methods can be greatly affected by human factors like conscientiousness, cautiousness and original thinking. The adherence to the inspection procedure, the experience and the mechanical comprehension are additional human factors. Those factors can be controlled by increasing the automation of the mechanized testing that will lead to higher reliability standards. The former can be accomplished by automated systems that can assist the inspection and the corresponding evaluation of the data. (Bertović, 2016)The liability of the NDT methods can also be affected in a smaller extent by environmental factors like temperature, noise level and humidity.

Non-destructing testing of polymer matrix composites can be expected to differ from the metallic materials. Composites have fundamentals differences with the metals and their alloys. In particular they are by far more anisotropic, exhibit lower thermal conductivity, higher acoustic attenuation and poorer electrical conductivity. Thus, different non-destructive techniques need to be used. The NDT inspection of the reinforced plastics is usually conducted using X-radiography, ultrasonic C-scan and neutron radiography. (I.G. Scott, 1982)

The atomic number of the elements in a material affect how the X-Rays are absorbed by the material. Specifically, in the composite materials attention must be given to the relative absorption coefficients of the fibres and the matrix. The radiography can be used to locate and identify voids but the debonding of the fibres or the resin and cracks that were caused by thermal contraction cannot be distinguished. In order to improve the information acquired using radiography the exposures must be made from at least two different directions. (Harris, 1980)

When the ultrasonic pulse propagates through an object, it is reflected or scattered from all the interfaces that separate regions with different acoustic impedance. (H. Jeong, 1995)In consequence, the C-Scan pulse is reflected or scattered from a defect, like a void, or from the far surface of the object that is under testing. The signal that is resulted from the echo is commonly received by a transmitting transducer that functions as receiver. The amplitude and the time required for the signal to travel form the defect to the receiver are the data used to yield information about the following: the dimensions of the specimen, its acoustic properties, the existence of non-planar surfaces and scratches. Delaminations and cracks normal to the ultrasonic wave beam will also be detected.

The ultrasonic C-Scan used ultrasonic waves that can be generated from piezoelectric transducers that can convert the applied voltage to mechanical vibrations. A medium, usually water, is then used to transmit the mechanical vibrations into the specimens. The propagation of the ultrasonic waves in elastic materials takes place by the displacement of the particles of the material. (A. Vary, 1977)

Some of the most commonly used non destructing methods are described on the table below.

Method	Main Principle	Applications	Advantages	Limitations
Visual Inspection	Uses natural or artificial lighting with a human eye or other photosensitive sensor	Various applications in many industries from raw material to finished product.	Low cost and little training required. Wide range of applications.	Only surface defects are detected. Requires accessibility and natural or artificial lighting.
Penetrating fluids	Liquid with visible or fluorescent paint spreads on surfaces and enters discontinuities through the capillary effect	Theoretically in any solid non-absorbent material with an uncoated surface. Used in non-porous materials. It can be used for welding, pipe casting, aluminum fittings, turbine impellers, gears etc.	Relatively easy to use and cheap. Very sensitive and flexible. Minimum training required.	Detects imperfections that reach the surface only. It requires a relatively smooth and clean surface. It does not specify the depth of discontinuities. Requires accessibility and natural or artificial lighting.
Magnetic particles	The object is magnetized and very small ferromagnetic particles are spread on the surface in alignment with the discontinuities.	All ferromagnetic materials. For superficial and minor sub-surface discontinuities.	Relatively simple to use. Cheap equipment / materials cost. Quite sensitive and fast	Detection is limited by field strength. Only for surface and some sub-surface defects. It requires a relatively smooth and clean surface. Removal is usually required after the end of the test. Ferromagnetic materials only. It does not specify the depth of discontinuities.

Radiography	γ or x rays penetrate the subject in question and trace their imprint on a special film.	Almost every material and geometry can be controlled.	Provides permanent log and high sensitivity. Volume control.	Thickness constraints depending on the density of the material examined. Detectability of imperfections depending on their directionality. Dangerous due to radiation. Decreased sensitivity with increasing thickness
Ultrasound	Ultrasonic waves are produced by special sensors and travel within the material. Defects affect the characteristics of propagation	Most materials can be controlled as long as they do not have high roughness and complex geometry. It is also used to determine thickness and mechanical properties.	Accurate results of high sensitivity. Information on thickness, depth and geometry of imperfections. Accessibility on the one hand.	Contact is usually required. Sensitivity dependent on main sensor frequency. Non-permanent log file (usually). Troubleshooting materials with very high damping, surface roughness and complex geometry. Requires coupling agent.
Streams	Located electric fields are produced in a conductor by electromagnetic induction.	All electrically conductive materials can be controlled. Surface and sub-surface defects can be detected.	Fast, flexible, sensitive. It does not require contact. Good automation.	Demanding to understand the variables that affect it. Low penetration depth (typically 5 mm). Indications

		Tubes, sliding bearings, aircraft components, transmission shafts.		affected by uncontrolled factors.
Thermography	Temperature changes on the surface of the specimen using thermal sensors.	In most materials and fittings that the temperature changes are related to the operating condition. Thermal conductivity	Very sensitive even to small temperature changes in small or large areas. Provides permanent recording.	Not for thick pieces. Surface evaluation. High specialization is required.
Acoustic Emission	Detection with special elastic wave sensors that propagate as the defects progress.	Tubes, pressure vessels, welds, composites and structures under load.	Large Surface Inspection. Possible prognosis of failure.	Sensors in contact with construction. Many sensors for fault detection. Requirement in signal processing.

Figure 4: Summary of non-destructive methods

1.6 Impact testing in Composite materials

The impact test is a technique for determining the behavior of a material subjected to shock loading in bending, tension and torsion. This test is designed to examine how a specimen from a known material responds to a suddenly applied stress. The impact test is mostly used to examine the toughness of composites, metals, polymers and ceramics. More details will be referred in chapter 4.

1.6.1 Low velocity impact devices

The machines that are currently used for simulating a low velocity impact response of composite materials include the falling weight fixtures like the Gardner, the Izod and Charpy

pendulums and hydraulic machines built to perform both out-of-plane and in-plane testing at low velocities as well as drop dart tests. (Cantwell, 1991)

1.6.2 Influence of constituent properties on the impact response of composite materials

The way that a composite material will deform and fracture depends on the properties of its constituents, the fibres, the matrix and the interphase region. Optical and scanning electron microscopes, as other techniques that will be discussed later, have been used to identify the number of failure mechanisms in polymer matrix composites that are fibre- reinforced. The failure mechanisms include interlaminar matrix cracking, longitudinal matrix splitting, fibre and matrix debonding, delamination, fracture and pull out of the fibres. Low fracture energy usually leads to fracture of the matrix or the interphase region, where higher energy fracture leads to fibre cracking.

The figure below presents the experimental data gathered from Chamis and Sinclair plotted as a function of the energy that the fibres are capable of absorbing that is determined by the energy under the static tensile stress/strain curve. (C.C. Chamis, 1985)An investigation of the data shows that there is possibly a connection between the two parameters, with materials that have fibres with greater strain energy absorbing capabilities presenting Izod energies. This technique can be used as a tool for evaluating the resistance in impact of composite materials.

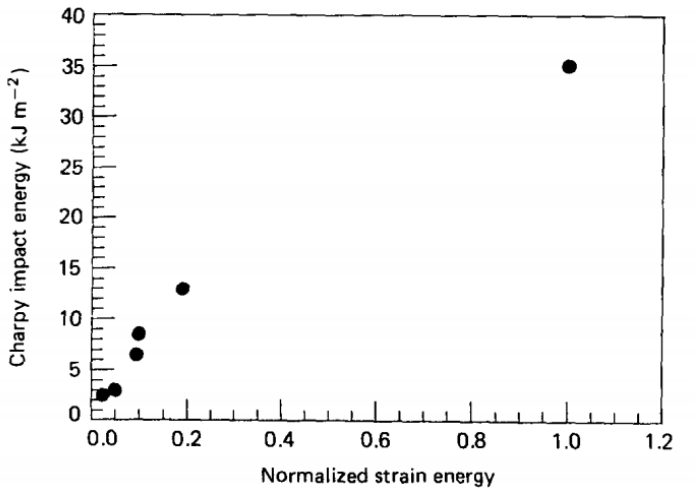

Figure 5: Variation of Charpy impact energy with normalised strain energy capacity of fibres [10]

2 Introduction to the Experimental Methods

The pipes that are used in gas and oil industries have dimensions that make it difficult to test in a laboratory. Conducting all the experiments in a full scale significantly raises the cost and the complexity. Transferring the full-scale specimens in the laboratory requires the use of additional personnel and more space. Furthermore, the testing machines need to be big enough so that the specimens can be tested. Thus, the use of a different approach is required. In industry, the first step is to conduct the non- destructive experiments with many small- scale coupons. Then, the same but fewer experiments take place but with medium scale coupons. The last step involves testing either full- scale or large- scale coupons in compatible more advanced machines is required. This approach is the most commonly used by the aerospace industry for evaluating and testing big parts. (M.O.W. Richardson, 1996)

In this study, the pipes that are going to be tested will be replaced with sections of pipes in order to decrease the time and the complexity of the experiments. In addition, determining if the curved sections of the pipes can be simulated with flat samples is of great importance but the effect of the curvature is out of the purpose of this study.

The impact tests will be carried out in pipe sections with random voids content. Then, the damage detection will be observed with the use of ultrasounds. This method will give a generic illustration of the void content, as well. The next step is to more accurately measure the void content of the specimens. This will be done with resin- burn off tests. In this method the resin is been volatilized and the specimens are being weighted prior and after the test. A more precise qualitive image of the void content can be obtained through advanced optical microscope. With this method, an effort will be made to investigate if there is an extent linking between the voids in the damaged area. The linking between the voids is very important to be considered, since it could constitute the start for a delamination and the failure of the structure.

In all the experiments pipes that are used in the Gas and Oil Industry have been used. These pipes have provided by the Wavistrong and are made of glass reinforced plastics. The type of the reinforcement is glass type C. This type is been suggested for structures that high resistance to corrosion is been required. The resin that was used is epoxy resin. The glass fibres are helical winded under $\pm 55^0$. In the following table, the properties of the pipes are shown. The thicknes of the pipes was 8.5mm and their length was 1.2m.

Property	Value
Axial tensile strength	65 N/mm^2
Axial tensile modulus	10500 N/mm^2
Hoop tensile strength	210 N/mm^2
Hoop tensile modulus	20500 N/mm^2
Shear Modulus	11500 N/mm^2
Axial bending strength	80 N/mm^2
Axial bending modulus	10500 N/mm^2
Hoop bending strength	90 N/mm^2
Hoop bending modulus	20500 N/mm^2
Poisson ratio axial/ hoop	0.65
Poisson ration hoop/ axial	0.38
Density of the fibres	2.52 gr/mm^2
Density of the resin	1.60 gr/mm^2

Figure 6: Mechanical Properties of the pipe

In the following picture are shown the pipes that were used in this study.

Figure 7: Pipes that were used in the experiments

Since, no full- or large- scale experiment was carried out, these specimens were cut in smaller specimens. Initially, they were cut in 150*150 mm specimens and then, depending on the nature of the test, their size may have been further decreased. For the sectioning of the pipes, a diamond cutter has been used. One of the difficulties that were faced during the cutting of the specimens was the curvature of the specimens. The diamond cutter has been manufactured to cut flat specimens. In the case of the curved specimens, during the cutting, the specimens has the trend to move upwards. So, a very high and downwards load should be applied on the upper surface of the specimen by the hands of the user. This high force in combination with the glossy surface of the specimens, could lead to unintentional accidents because the fingers that were pushing down the specimen could glide from the surface and end up on the wheel. So, extra carefulness, slow movements, cutting gloves, glasses and a waterproof lab- coat and a mask were used during this procedure.

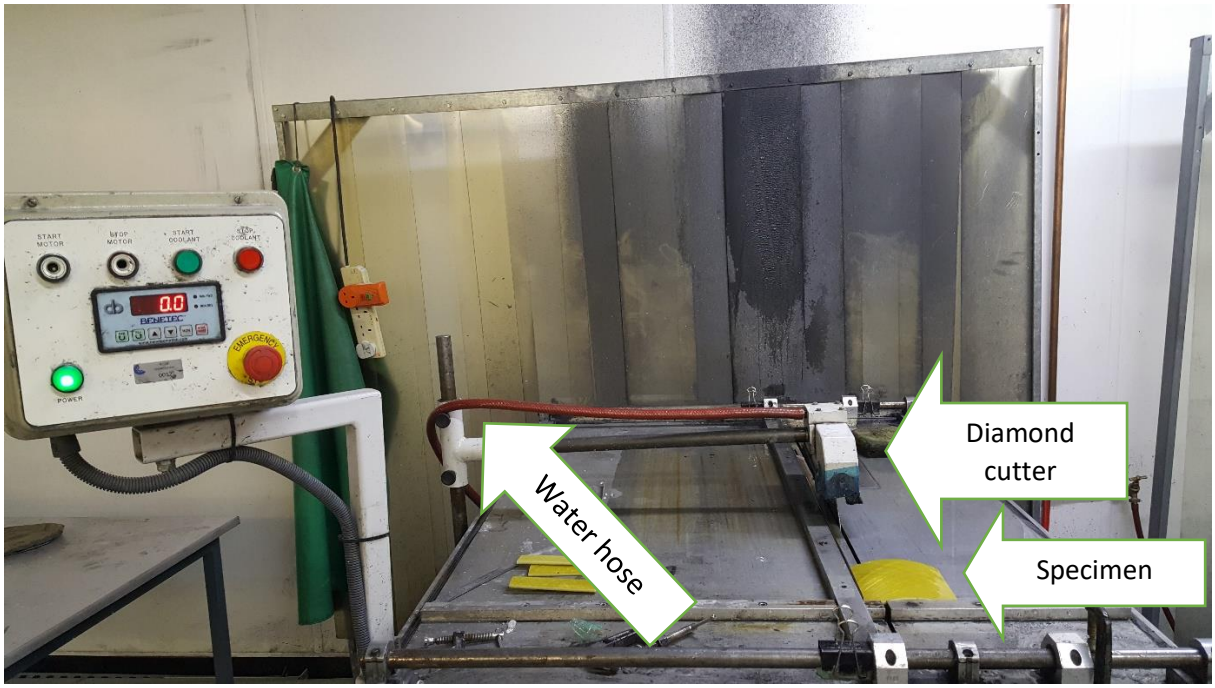

Figure 8: Diamond cutter

It is also important to mention that the specimens have never come in contact with naked skin, only with protective gloves. That' s because the glass fibers can easily penetrate the skin and cause itching and even irritation.

3 Impact testing

The purpose of these test methods is to determine how the void content affects the damage resistance of a fiber-reinforced polymer matrix composite after a low speed weight-drop impact event. However, in this study, the test methods were used to create impact damage to the specimens that was then used to examine the extend of the damage and the linking between the voids for different void contents. The Test Methods were based on the Standard D7136/D7136M – 15 which is for flat composite plates. The damage resistance properties examined in this standard are highly dependent upon factors such as the geometry of the specimens and the impactor, the mass of the impactor and the boundary conditions. The test methods had to be modified, since, the specimens were curved and not flat.

A lot of studies have studied the response of flat specimens under impact event. However, the papers that have released regarding curved specimens are very limited. Many factors have been investigated, like the thickness, the lay-up and the material. In example, the thicker the laminate the more resistant to impact event is. (Francisco C., 2015).

3.1 Summary of Impact testing

The impact event is performed by dropping a weight in a symmetric, balanced laminated plate. The drop-weight has a striker tip that causes a concentrated, out of plane impact. The impact for the flat specimens is perpendicular to the plate, while on the curved plate it is perpendicular to the plane parallel with the top of the plate. The damage resistance can be judged based on the size of the damage and the type of the damage. The damage and the damage response are a function of the test configuration, so different specimens can be compared only when they were tested under identical test configurations.

3.2 Method

The rigid base (shown in the picture below) had the specifications defined in the standard. The top plate (fixture base) that the specimens are placed was 25 mm thick made and was made of aluminum. The dimensions of the cut-out of the top plate were not taken into consideration. The reasons will be described later in this chapter. The fixture base was aligned with the base plate with the use of 4 bolted supports, with 19 mm radius and 300 mm long. The base plate was 13 mm thick, 320 mm by 320 mm and made of aluminum.

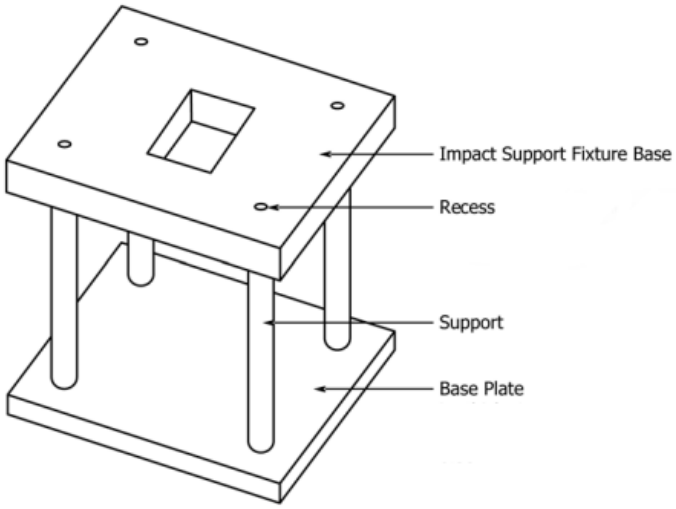

Figure 9: Rigid Base

In the experiments with flat specimens, the specimen is placed on the fixture base and fastened with the use of 4 clumps. However, with the curved specimens, this procedure was not possible. As shown in the picture below the area that the rubber tip of the clumps comes in contact with the specimen is elevated in the curbed specimens. As a result, the clumps can't be locked in position (see picture above) and the specimen can't be fastened. In addition, the surface of the flat specimen comes in contact with the plate of the impact machine while on the curved specimen the surface is not supported (see picture above) which could lead in different distribution of the impact energy than the expected one. In order to solve those 2 problems a support fixture was designed.

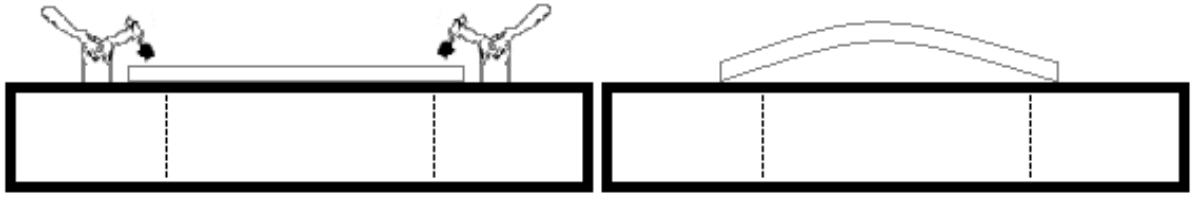

Figure 10: Flat and curved specimens placed on the plate of the impact machine (the dimensions of the specimen and the fasteners are not proportional)

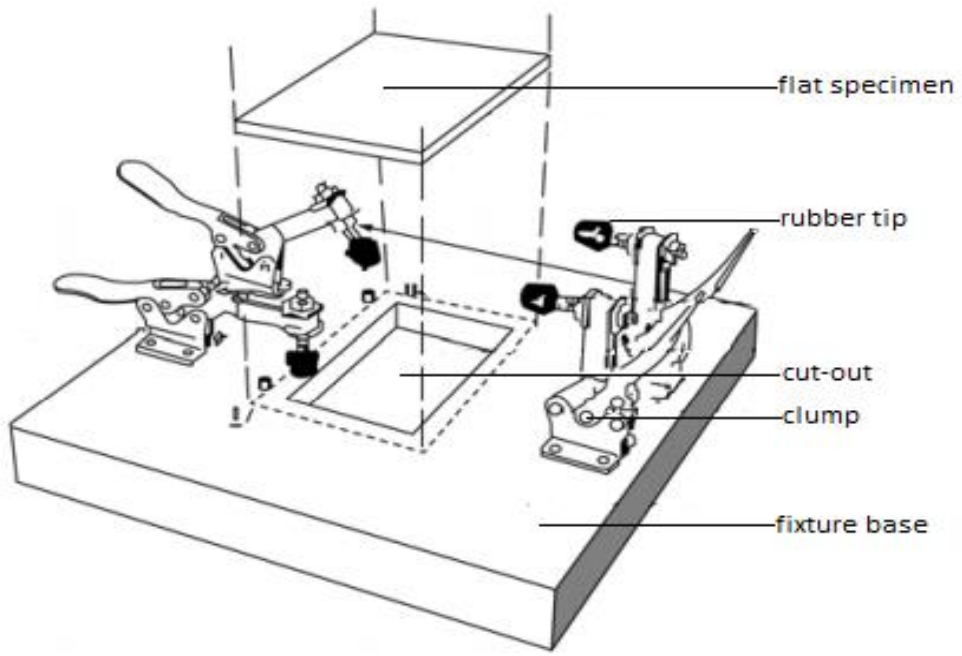

Figure 11: Impact support fixture (Source: ASTM D7136)

The mechanical design shown below was exclusively made for the purpose of this study using Solidworks 2014.

The new fixture had to fully support the surface of the flat specimen that comes in contact with it, in order to simulate the boundary conditions of the tests with the flat specimens. For this reason, the upper surface of the fixture was designed with the same curvature as the specimens. The specimens were fastened on the fixture with a non-traditional technique. Four bolt and four washers were used to fasten the specimen. Before placing the specimen, the bolts had to be unscrewed but not completely, so that the specimen could fit to slide below the washer. Then the bolts were tightly screwed in order to fully support the specimen. The bolts were not completely unscrewed each time before placing the specimen in order to save time but at the same time to protect the threads of the fixture for later use.

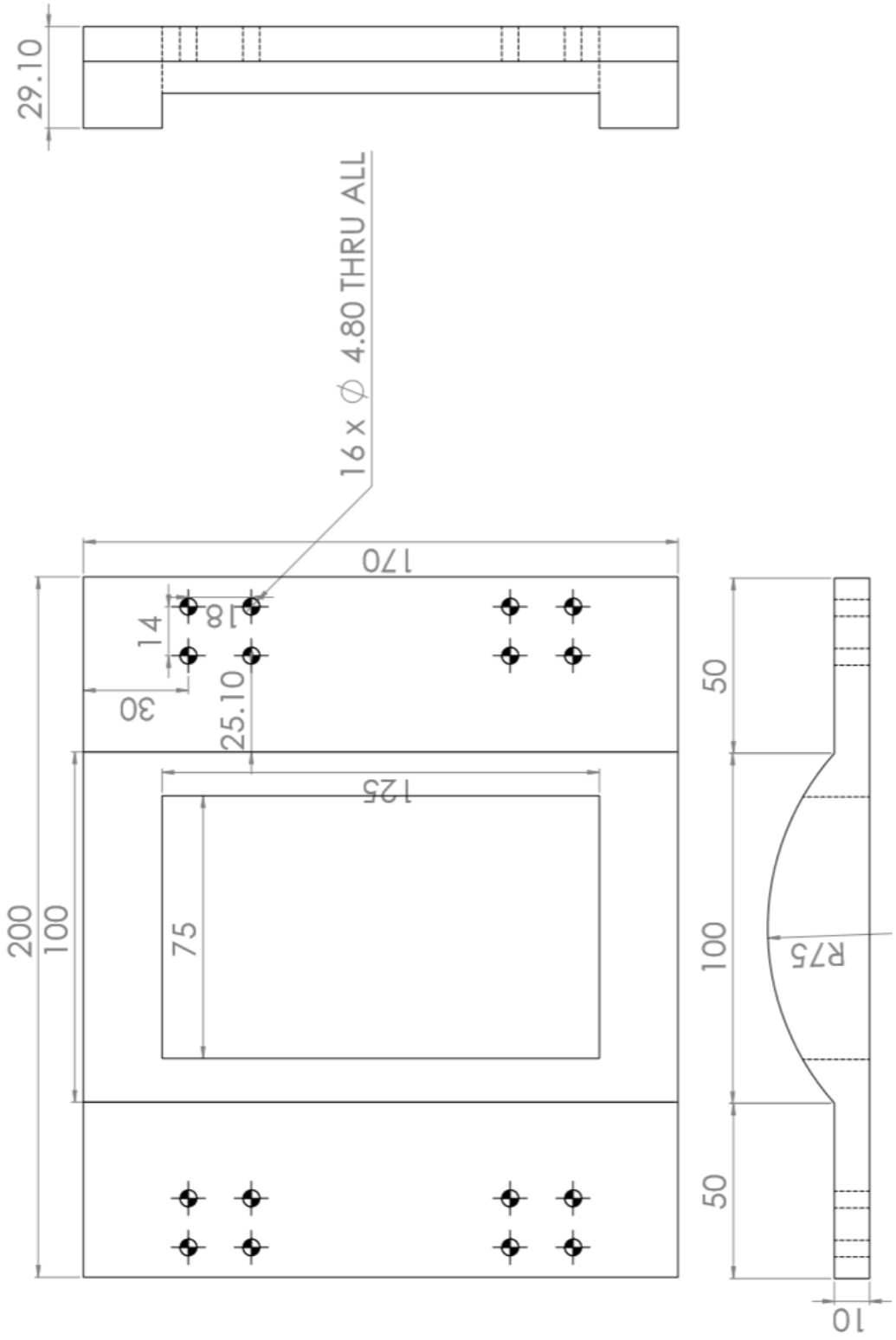

Figure 12: Mechanical Design of the Custom Fixture made on Solidworks

. The part was made from a block of aluminum. Removing the aluminum from the center of the block using a CNC machine would have taken a lot of time so a large drill press was used (see picture below). Two different drills were used. The initiation of the hole became with a 3/4'' Twist Drill at 380rpm and the rest of the material was removed with a 1-5/8 Twist Drill at 230rpm.

Figure 13: (Left) 3/4'' Twist Drill, (Right) 1-5/8 Twist Drill

Then the aluminum block was formed to the final design with the use of an CNC Machine

Figure 14: Completed Custom Fixture

3.3 Errors and Interferences

The damage response of the specimens (laminated plates) to out of plane drop-weight impact is influenced by many parameters like the sequence of the plies, the thickness of the plies and the specimen, the geometry of the tip of the striker, the mass of the impactor, the boundary conditions the environment and more. Thus, if comparisons are to be made between the specimens, the configurations of the tests, the specimens and the conditions need to be identical.

If the impact force is not perpendicular to the plane of the laminated plate, then the results can be greatly affected. The formation of the impact damage in the composite specimens that are used in this study is also affected by their geometry. Differences in the stacking sequence, the thickness of the plies, the size and the shape during manufacturing were considered and

the specimens that deviated a lot were excluded. The characteristics of the fixture and the impact device are variables that affect the tests. The tests lasted for several days so attention was given so that those variables would not change significantly.

3.4 Conditioning and Test specimens

No explicit conditioning process was conducted; thus, the specimen conditioning process was reported as unconditioned and the moisture content unknown.

Based on the standard five specimens per test should be tested unless results could be gained through a smaller number of specimens. Initially three specimens were cut for each test and in case that the results were not consistent more specimens would have been cut. Based on the data collected from the three specimens of each test it was concluded that there was not need for more specimens to be tested. The data and the curvatures of each test had small variations with each other.

3.5 Impact Tests

Initially, an impact tower (CEAST 9350) with a rigid base as described in the chapter 3.2 was chosen for the tests. However, due to calibration problems a different drop tower had to be used. Both are shown in the picture below.

Figure 15: (on the left) initial impact tower, (on the right) impact tower used for the tests

The rigid base that was used to place the fixture as shown in the picture below. Two fasteners had to be used to fasten the fixture on the rigid base of the impact tower (see picture below).

p

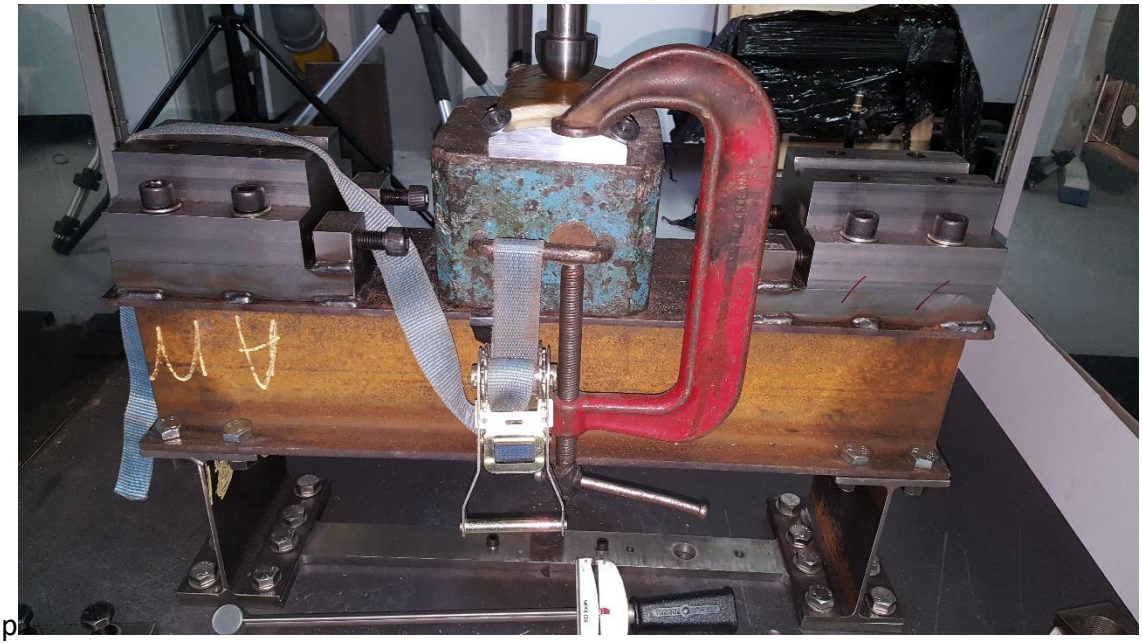

Figure 16: Fixture fastened on the rigid base

The specimen was fastened on the fixture with the use of bolts and washers as described in the chapter 3.2. Prior to testing the actual specimens, a specimen was tested and closely observed in order to verify the effectiveness of this fastening method. No movement was detected between the specimen and the fixture, so this fastening method was accepted. It is worth mentioning that the bolts had to be screwed using high forces.

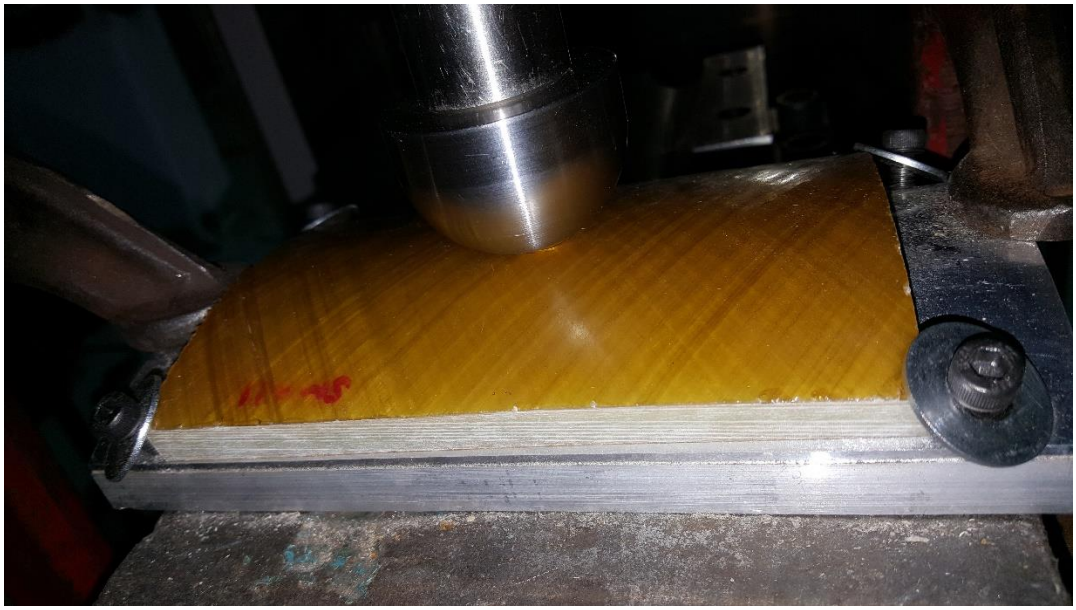

Figure 17: Specimen fastened on the fixture

Two categories of specimens were examined. Those with low void content and those with high void content. Two impact energies were used for the impact events, 10 and 20 Joules. For each scenario were used 3 specimens so in total 12 specimens were used.

As previously mentioned, the results of each specimen of the same scenario were in most of the cases similar so in the diagram below its scenario is presented with one curve. The curves were made from the average of the individual curves of its specimen. As 'Low' are described the specimens with low void content and as 'High' those with high void content. Calculating the void content with the burn-off resin technique is a destructive method so those experiments had t be conducted after the impact tests.

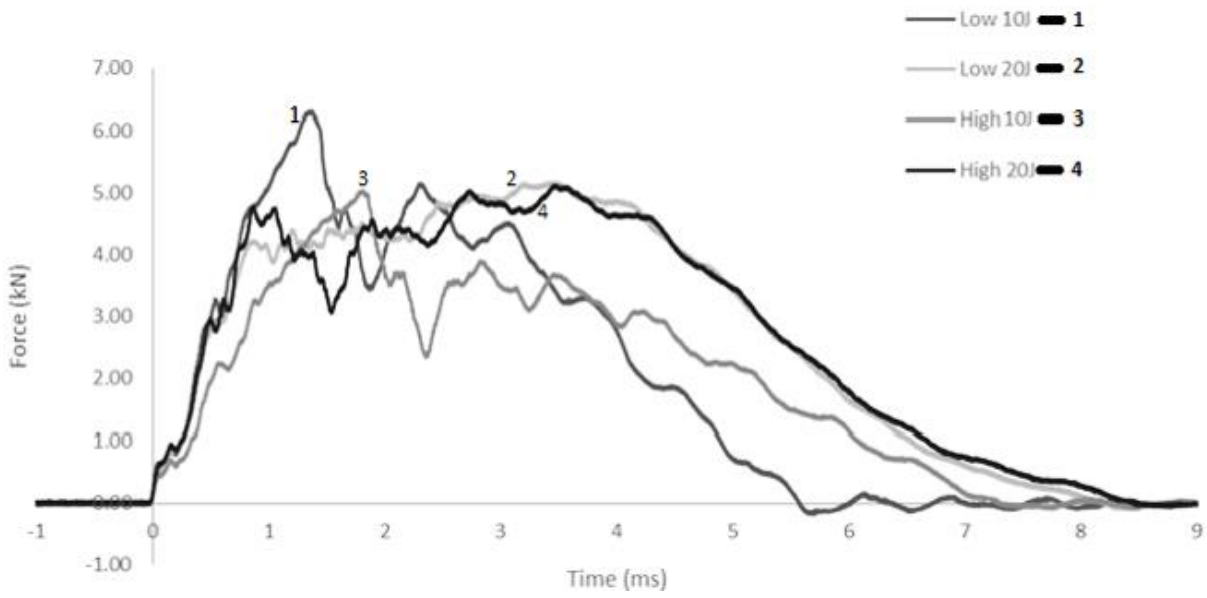

Figure 18: Time-Force during the impact event

In the figure above the impact event starts at 0ms time and finishes when the force is zeroed. The area below that is formed between each curve and the x axis is the impulse.

3.4 Conclusions

In the diagram above the 4 curves of the Low and High void content specimens after 10J and 20J impact energies can be seen. The specimens that were tested under 20J impact energy (curves 2 and 4) presented similar behaviour independently to the void content. The specimens that were tested under 10J impact energy did not appear to have similar behaviour.

From the results above the following can be concluded. When the impact energy is low the behaviour of the specimens cannot be predicted, and it is different every time. For higher impact energies the specimens behave in a more consistent way and therefore the curves were similar. That means that the curves that correspond to the 20J specimens are more close to each other compared to the curves that were impacted with 10J impact energy, whose between distance is bigger. By examining the high impact energy curves, it can be observed that the void content did not appear to significantly affect the behaviour of the specimens

4. Ultrasonic C-Scan

The ultrasonic C-scan is the main method for inspection of composite materials because it provides reliable and accurate results in a very short time. At the same time, it is a very safe method to use. For those reasons, C-scan was used as the initial method, used to acquire a general idea of the size of the damage of the impacted specimens.

The ultrasonic machine that was used in these experiments was the Midas NDT C-scanner. It can be seen in the image below.

Figure 19: C-scan machine used for the experiments

4.1 Method

The specimens had to be fastened in order to restrict any movement. The jet of the water hits the specimens in the same area from both sides, so the applied forces were balanced. Thus, there was no need to fasten the specimens very strictly.

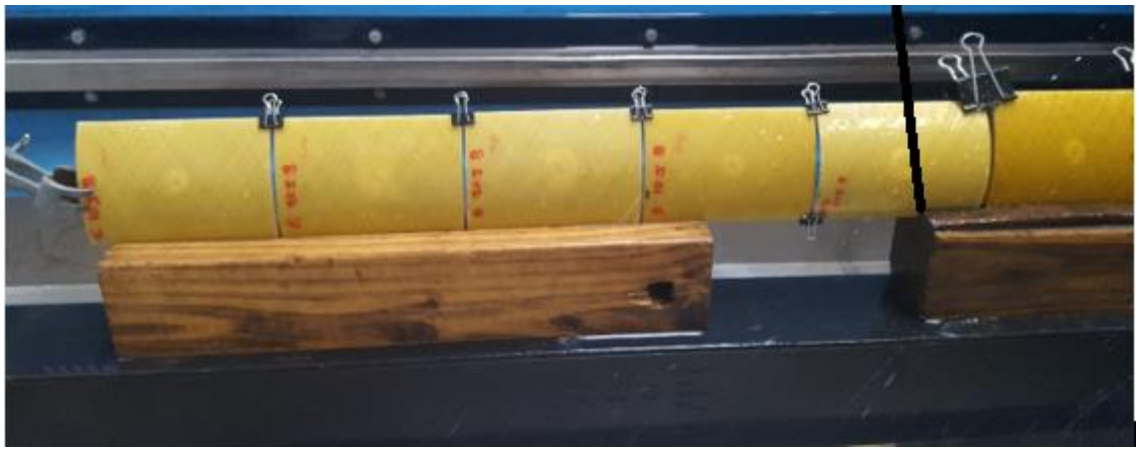

Figure 20: The specimens fastened on the C-scanner

The specimens were placed on two pieces of wood. Those pieces had a channel with the same thickness as the specimens. The lower side of the specimens was placed inside the channel of the wood. The specimens were fastened with each other by using clips. There were 12 specimens, so a lot of effort was given to fit 6 specimens and this was achieved by leaving a gap between the two wooden pieces.

Initially, the system had to be calibrated based on the atmospheric conditions of the room. The humidity and the temperature of the air change the results of the scan. For this reason, all the tests were conducted during the same day, without leaving any dead time during the 2 scans since the temperature slightly changed inside the room during the day. The starting and ending points of the scan had to be defined. The starting point was on the bottom left side of the setup and the ending on the top right. The specimens were scanned using a 1MHZ probe, as shown in the picture below.

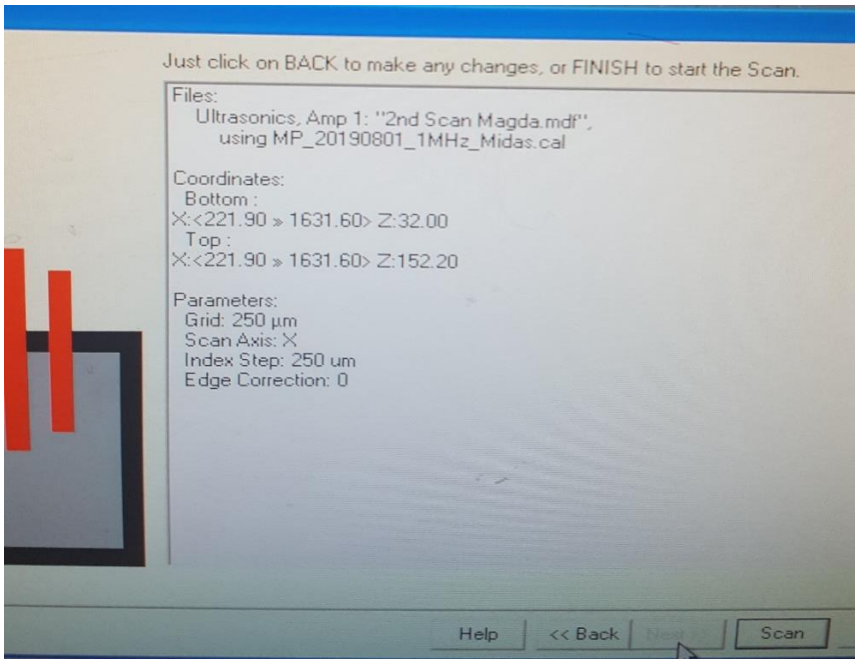

Figure 21: Settings of the C-Scan

4.2 Results

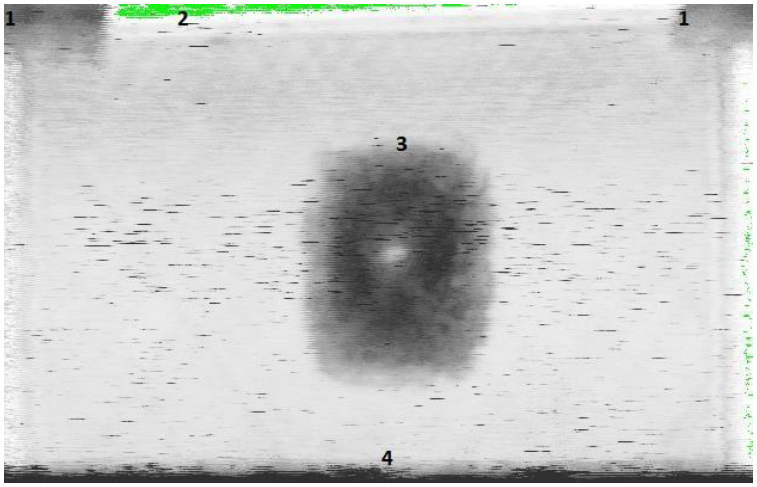

Figure 22: Different areas of the scan

In the scanned specimen there are presented a lot of different areas as shown in the picture above. The dark areas presented with the number 1 are the locations were the clips were attached. It is normal that the area is darker and there are less details of the composite since the clip was on obstacle for the transmitted signal. The green area presented with the number 2 is not an area that belongs to the specimen, but it is air. In the air the signal can be transmitted extremely easily, thus almost the whole signal passed for the transmitter to the receiver and that lead to a green area. The 3 area is where the impactor hit the specimen. They are shown with the number 4 is where the specimen was placed inside the wooden channel. The wooden beam was very thick and this is why almost no signal passed through and the area is very dark.

Below are shown the results using the 1Mhz probe. One specimen is shown for each case. It can be easily observed that the scan on the specimen with high void content that was impacted with 20 Joules doesn't have appropriate resolution. Most of the damaged are is shown as black which makes it impossible to draw detailed conclusions. For this reason, a different probe (transmitter) was used to scan the specimen. The specimens had small thickness so using a probs with high frequency was not a problem since the signal could pass through. So a 0.5 MHz probe was chosen. All the observations were made on the specimens tested in 0.5MHz.

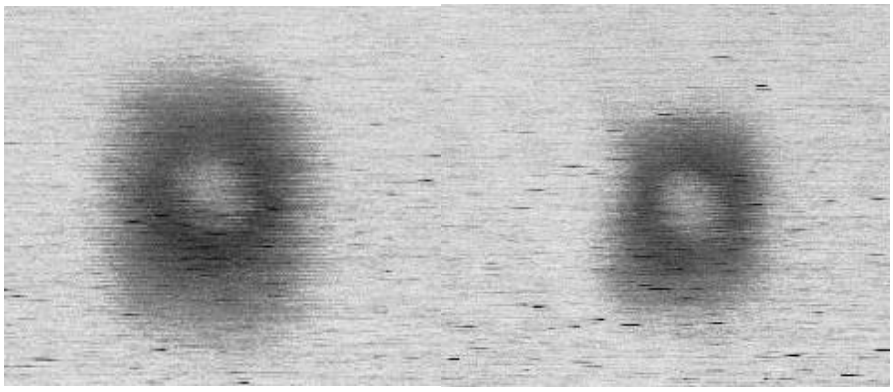

Figure 23: 10J Impact energy, 1MHz, High void content on the left and low on the right

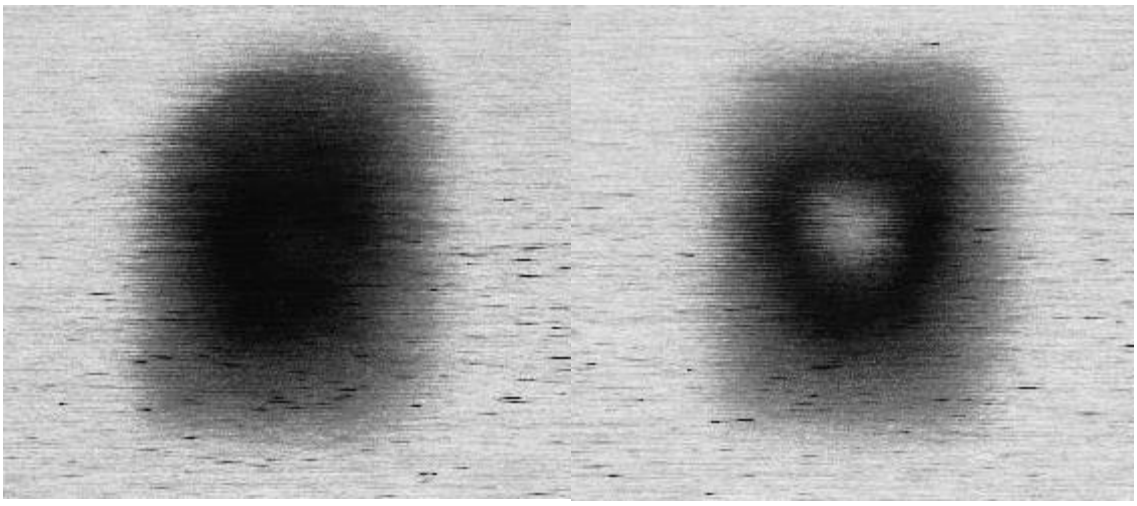

Figure 24: 20J Impact energy, 1MHz, High void content on the left and low on the right

All the pictures shown of the damaged areas have the same scale so that accurate observations can be made. As expected, the damaged area of the 20J tests has a significantly bigger size than the 10J tests. It can also be observed that the specimens with higher void content had a more extensive damage than those with lower void content within the same impact energy. This behaviour was also expected but with less certainty.

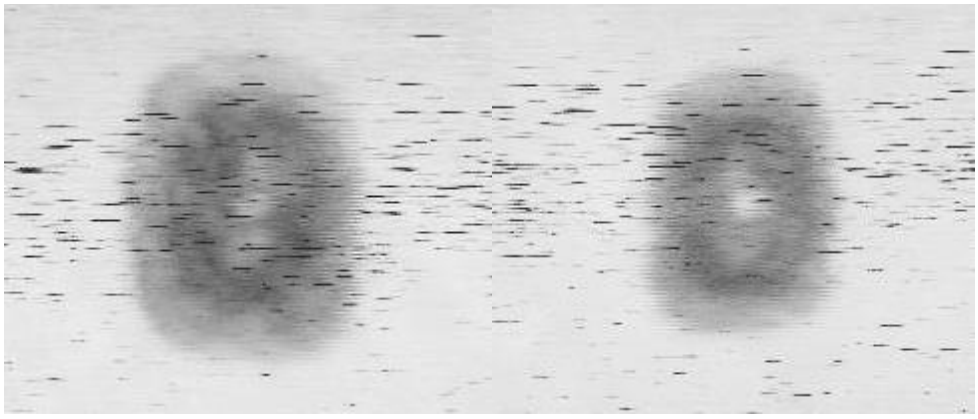

Figure 25: 10J Impact energy, 0.5MHz, High void content on the left and low on the right

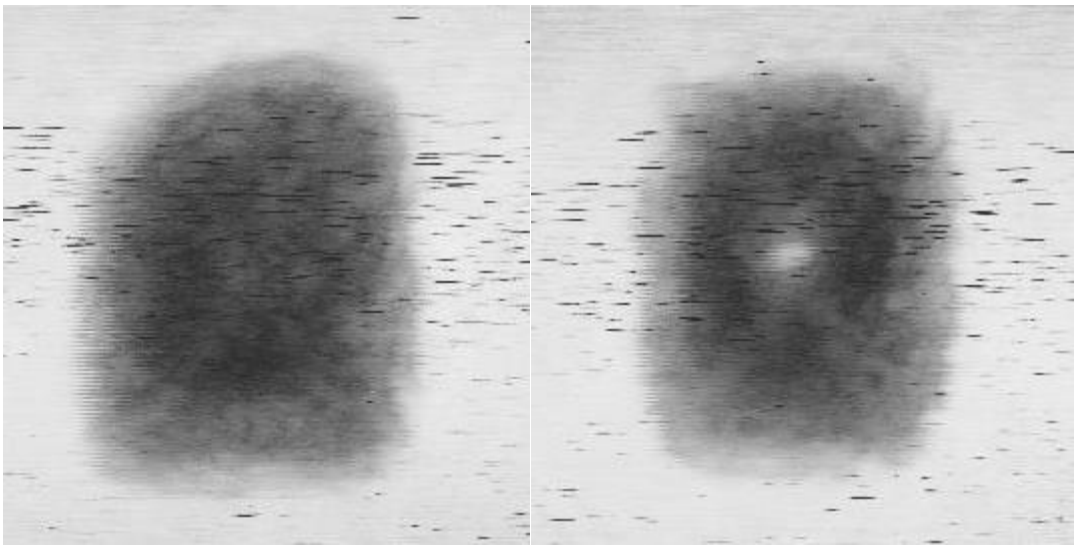

Figure 26: 20J Impact energy, 0.5 MHz, High void content on the left and low on the right

4.3 Conclusions

It can be stated with certainty that the void content significantly affects the behaviour of the glass fibre reinforced composites under low velocity impact events. A higher void content means lower impact resistance that leads to a more extensive damage.

5 Calculation of Void Content through Burn Off Resin Tests

The purpose of the burn off resin tests is to measure the void content of reinforced plastics or composites. The tests can be applied to composites for which the effects of ignition on the individual materials of the composite are known. The test method cannot be applied to composites of which the effects of ignition of its components, matrix and reinforcement, are unknown. Composites that have resins that do not burn off completely or reinforcements that may gain or loose weight belong to the previously mentioned category. When testing the weight loss of individual materials usually, but not necessarily, the results are the same as when all the materials are tested combined.

The mechanical properties of a composite can be significantly affected by the void Content. Higher void contents can lead to lower fatigue resistance, higher susceptibility to water penetration and weathering, and increased scatter or variation to its strength properties. Thus, the knowledge of the void content is important for the oil and gas industry pipes that are made of composite materials.

5.1 Summary of Burn off Resin Tests

The first step is to measure the density of the composite. Then, the density of the resin and the reinforcement of the composite are measured separately. After, the resin content is measured, and a theoretical composite density value is calculated. This value is compared to the measured density of the composite. The void content is then measured by the difference in densities. Generally, a value of 1% indicates a composite of very good quality, while a poorly made composite can have a much higher void content

5.2 Method – Burn off Resin Test

The standard that was used in order to conduct the burn off resin tests is the ASTM D2734-16. The D letter indicates that this standard was developed and published by the American

Society for Testing Materials, while the number after the designation shows the year of the latest revision.

This standard describes three methods, that will be described in the next chapters, that can be used to measure the density of the composite. Based on the standard, the density of the Resin and the Composite must be measured in specimens that have no bubbles and that were cured with conditions (heat, pressure, time) similar to the conditions under which the composite was cured. When the density measurements are provided by the manufacturer, they are acceptable as long as they are certified for each batch. In this study, the density measurements were provided by the manufacturer, however the technique that was used to measure the densities is unknown. For this reason, effort was made to measure the density of the matrix and the fibers. However, there was access only to raw fibers and not to resin. The results of the experiments that were conducted to measure the density of the fibers, were very close to those provided by the manufacturer. More will be discussed later.

5.3 Errors and Interferences

Before conducting the experiments, it is essential to take into consideration possible errors and interferences that could significantly change the results.

When measuring the density of semi-crystalline plastics, like polyetheretherketone (PEEK) and polyphenylene sulfide (PPS), the crystallinity that is present in the composite can cause an interference that could lead to significant variations. For those plastics, the value of the density that is used for the calculations must be the actual density of the resin in the composite. The extend of the crystallinity can be measured by techniques like the differential scanning calorimetry or with X-ray diffraction. The composite that is examined in this study has as a matrix with low crystallinity based on the specifications of the manufacturer and thus its effects are limited and not taken into consideration.

The density of the resin of the composite is assumed to be equal with the density of the resin in a large cast mass. However, this assumption is not completely accurate since when the resin is cured while inside the composite, it interacts with the fibers. This causes differences in curing, pressure, heat and in the molecular forces between the interface of the resin and the reinforcement which can result to different density than the one of the large cast mass. In most cases the density of the bulk resin is lower, which causes the void content to appear lower.

The density of the resin, in these test methods, is assumed to be the same in the composite as it is in a large cast mass. Even though there is not a realistic way to avoid this assumption, it is not strictly correct. Differences in heat, pressure and curing, and the molecular forces from the reinforcement surface all together change the composite resin density from that of the bulk resin density. The usual change is that the bulk density is lower, making the void content to seem lower than it really is. How the lower or higher void content affects the integrity of the results and the conclusions will be discussed later in this study.

The error mentioned above for a composite with void content would lower the value of the void content from a true 10% to 9.7%, for example, which is not a significant amount. For a composite with low void content, the value could be lowered from 0.5% to 0.4%, for example, which is a very big error. This means that as the void content becomes lower, the importance of the error in the density becomes higher. The specimens tested in this study have a high void content, thus the importance of the error in the density is limited.

5.4 Conditioning and Test conditions

The conditioning of the test specimens and the test conditions that are used in the ASTM D2734 - 16 and by extension in this study are described in the ASTM D618 - 13. The selection of the appropriate ASTM for the Conditioning and test conditions was made using the ASTM D4000 - 16. Based on the materials that the specimens consist of the D4000 suggests using the D618 - 13.

Based on the D618 the test specimens should be conditioned at 23 ± 2°C and 50 ± 10% relative humidity for more than 40h prior to the burn off resin tests. The burn off resin tests should be conducted in a standard laboratory atmosphere of 23 ± 2°C and 50 ± 5% relative humidity.("Standard Practice for Conditioning Plastics for Testing,")

The specimens prior to the tests and during the tests were located in the same room. The temperature and the humidity were measured using a Digital Indoor Hygrometer Thermometer, Room Thermometer. Based on the manufacturer of the accuracy of the device is ±1℃/±5%RH. The accuracy of the temperature is higher than the required, however the accuracy of the humidity is the same 5%. Ideally a hygrometer with higher accuracy should be used. The temperature was measured 24 ± 1°C and the relative humidity 52 ± 5. The humidity of the room deviated from the suggested humidity but in a small degree. Changing the humidity of the room was not possible so this small deviation was accepted.

5.5 Test Methods - Measuring Density

In the ASTM D2734 there are described three test methods to measure the density, methods A, B, and C. Only the method A will be described since it is the one that was excusively used during this study.

5.5.1 Method A - Measuring the Density

The density in the D2734 for the Method A is measured using the test methods of the ASTM D792. This method was used to measure the density. In brief, the mass of the composite is measured in the air. Then the composite is immersed in a liquid, its apparent mass upon immersion is determined and then its relative density is calculated.

Based on the ASTM D772 - 18 the conditions prior to the tests and during the tests were those described in the previous sub-chapter. The samples used for determining the relative density (specific gravity) were representing the quality of product for which the data are required. For the impacted laminates, the samples were extracted from the undamaged area close to the damaged area. The laminates made of composites present a very big fluctuation in the distribution of the void content. Thus, it is crucial to measure the void content as close to the damaged area as possible.

Since the tests for the calculation of the void content constitute a destructive technique, the tests had to be conducted after the impact tests. The samples could not be extracted from the damaged area since the void content could not be calculated correctly there. The impact event introduced damage, including cracks and delaminations, which affected the number of voids in the area. The samples were extracted 40mm away from the end of the damaged area. However, the accuracy of this technique had to be validated. The fluctuations of the void content in the composite could lead to different void content in the damaged area, prior to the impact event, with that in the area from which the sample was extracted. For this reason, in the first 3 specimens, 4 samples were extracted (as shown in the picture below) from each specimen. If the samples from each specimen had identical void content, then the damaged area would initially (prior to the impact event) have identical void content too.

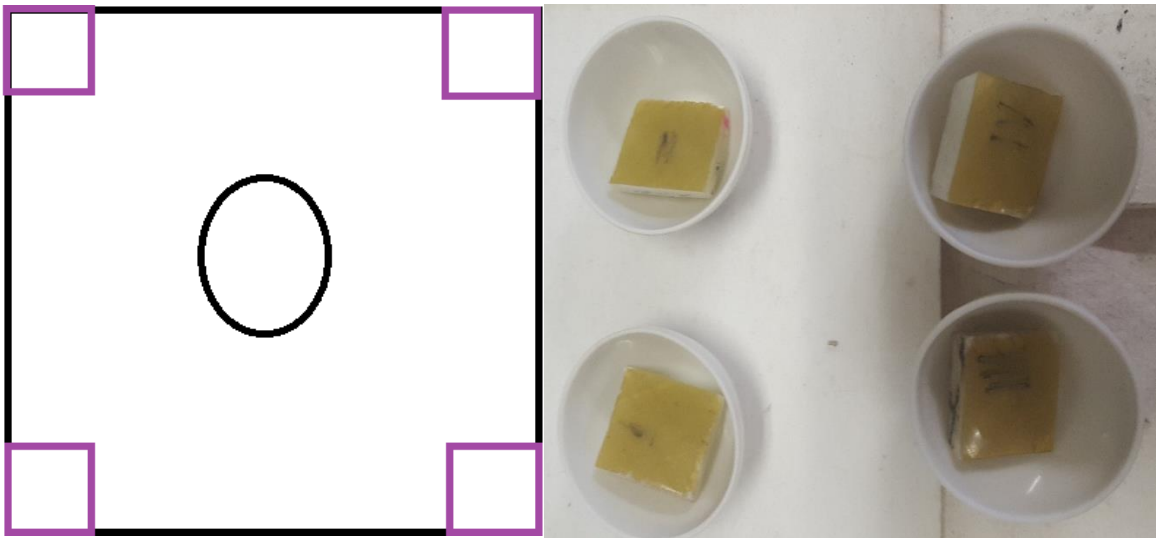

Figure 27: The extracted specimens from a damaged laminate

The extracted samples had 25 mm length and 25 mm width. The void content of the 4 specimens is shown in the table below:

	1st corner	2nd corner	3rd corner	4th corner
Void Content	11.8851 %	11.9548 %	12.0251 %	11.9526 %

Figure 28: Void content of the 4 corners of the impacted specimen

The method that was used to calculate the void content is fully explained in the chapter 5.7. The void content of the 4 specimens is very similar so it is safe to assume that the void content in the impacted area has very similar void content.

A balance with a minimum precision of 0.1mg is required for materials with densities less than 1.00g/cm^3 and minimum 1mg for all the other materials. The specimens had a density higher than 1.00g/cm^3, in average 1.930g/cm^3, so a balance with minimum precision of 1mg was required. The balance that was used had a precision of 0.1mg.

As liquid, that the specimens are immersed in, was used air-free and distilled water. The air bubbles were removed from the water by shaking the flask. The edges of the test specimens were smoothed using a 600-grit emery paper.

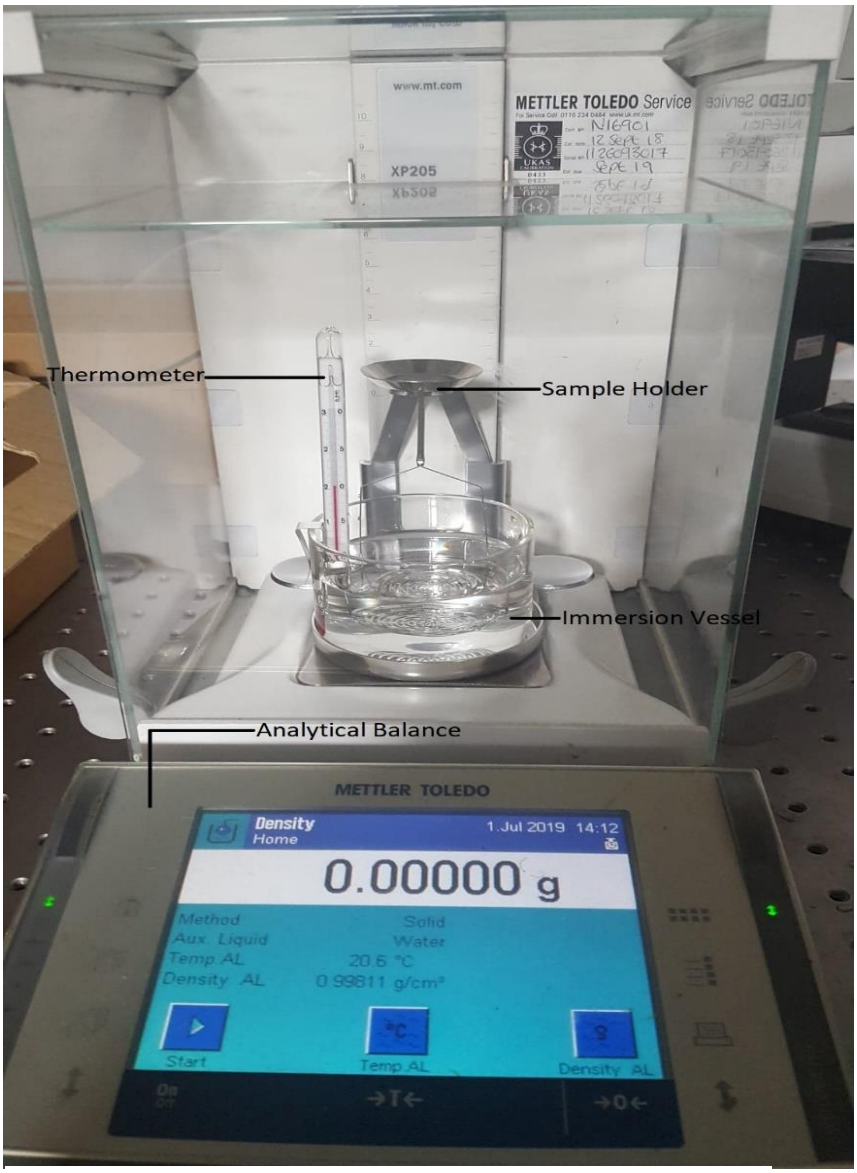

Figure 29: Balance

The thermometer used to measure the temperature of the water was readable to 0.1°C. The sample holder was corrosion resistant. The immersion vessel was a beaker for holding the immersed specimen and the water. There was no need to use a sinker since the density of the specimens is higher than 1.00, so they did not float on the water. The test specimens were a single piece of material and had shape and volume that would fit the sample holder. They were free from grease, oil and other foreign matter.

5.5.1.1 Procedure

The immersion vessel, the thermometer and the sample holder were placed inside the balance. The immersion vessel was mounted on the support and did not touch the sample holder or the specimen. Then a sufficient amount of water was poured inside the immersion vessel so that it would fully cover the immersed specimen. The water temperature was measured and recorded, and the scale calibrated. Then the specimens were weighted in the air. The next step was to place the specimen inside the water and remove any bubbles adhering to the sample holder or specimen by rubbing them with a tweezer. The bubbles did not keep forming so there was no need to use vacuum. Afterwards, the mass of the suspended specimens (apparent mass of specimen – b) was determined to the required precisions.

5.5.1.2 Calculations

The density of the specimens was determined based on the ASTM D792.40752.

The temperature of the water was not 23°C, so the density of the water at 24°C must be converted as follows:

$$M = \Delta D / \Delta t$$

$$D \text{ (conversion @ 23°C)} = \text{sp gr } t_a / t_w \times [997.5 + (t_w - 23) \times M], \text{ kg/m3}$$

$$\text{sp gr } 23/23 = D \text{ (conversion to 23°C)}/997.5$$

where:

M = slope,

ΔD = the difference between the density of the water for the lowest and the highest temperature tolerance,

Δt = the difference between the highest and lowest temperature tolerance that is recommended,

t_a = temperature of the air, and

t_w = temperature of the water.

In order to calculate the slope M (0.2367), the value of Δt and ΔD must be defined. Δt is equal to 4 as it represents the difference between the highest and the lowest temperature tolerance that is indicated in the standard, which is ±2. ΔD, which is equal to the difference in the corresponding densities of the water at 21*°C* and 25*°C, has been calculated based on the values of the following table. Thus,* ΔD= 997.9948 - 997.0480 = 0.9468. The temperature of the water was measured 24°C and the temperature of the air 24°C, both with a tolerance of ±1℃. Using the equations above the density of the water was measured 9997.2245. Using the table above the standard density of water on 24℃ is 997.2994, which is very close to the calculated value, thus the value of the table was used.

°C	D=/kg m^{-3}									
ΔD	0.0	0.1	0.2	0.3	0.4	0.5	0.6	0.7	0.8	0.9
21	997.9948	9731	9513	9294	9073	8852	8630	8406	8182	7957
22	997.7730	7503	7275	7045	6815	6584	6351	6118	5883	5648
23	997.5412	5174	4936	4697	4456	4215	3973	3730	3485	3240
24	**997.2994**	2747	2499	4456	2000	1749	1497	1244	0990	0735
25	997.0480	0223	9965[B]	9707[B]	9447[B]	9186[B]	8925[B]	8663[B]	8399[B]	8135[B]

Figure 30: Standard Density of Water

The next step was to calculate the specific gravity of the composite of each specimen using the equations that are shown below:

$$\text{sp gr } 23/23°C = a / (a + w - b)$$

where:

a = the apparent mass of the specimen without including the mass of the wire or the sinker, in air,

b = the apparent mass of the specimen (including the mass of the sinker if used) when it is completely immersed in the water and of the wire partially immersed in the water, and

w = the apparent mass of the totally immersed sinker (if it was used) and of partially immersed wire.

During the experiments no sinker was used. The mass of the wire, that was holding the specimen so that it will not come in touch with the immersion vessel, was excluded from the calculations by zeroing the balance prior to the immersion of the specimen. Thus, b=0 and w=the apparent mass of the specimen when it is completely immersed in the water.

Finally, the density of the composite was calculated using the equation below:

$$D^{24C} = \text{sp gr } 23 / 23°C \times 997.2994, \text{ kg/m}^3$$

W_{air} is the weight of the specimen in the air W_{water} is the weight of the specimen when fully immersed in the water. In the table below is shown the calculated density from 9 different specimens:

W_{air} (gr)	4.072	4.4587	4.6746	3.8378	4.2569	4.3549	4.1249	3.9452	4.02548
W_{water} (gr)	1.9706	2.1383	2.2643	1.857	2.0616	2.1091	1.9977	1.9107	1.94959
D_{comp} (gr/cm^3)	1.933	1.917	1.935	1.933	1.929	1.930	1.932	1.928	1.931

The value of the density of the composite was very consistent with an average of 1.9297 gr/cm^3. The specimens were extracted from different areas of the same 1m long piper, thus the consistency of the results proves the effectiveness of this method.

5.6 Burn off Tests

A number of resin- burn off tests were conducted in order for the weight of the fibers and the weight of the resin to be measured. In the resin burn off tests the specimens are inserted in an electric muffle furnace until the resin is fully volatilized. The specimens are been weighted prior and after the burning off test.

This test method can only be used when the material of the reinforcement does not lose weight under the test conditions and when the matrix is a material that can be decomposed

under the same test conditions. The glass fibres and the epoxy resin, that are used in this study, satisfy these two requirements.

This test method is hazardous. So, heat-resistant gloves and tong was used during the insertion and the extraction of the specimens to and from the oven. Also, the temperature of the specimens was carefully measured prior to direct contact with hands or surfaces that are nor resistant to high temperatures.

For the conduct of the test, platinum or porcelain crucibles are needed. Each specimen is placed in a crucible and then placed with it in the oven. By this way, it will be assured that there won't be any fibre loss during their transfer from the oven.

All burn off tests have been conducted in standard laboratory atmosphere at approximately 23^0C and 50% relative humidity.

Each specimen was weighted prior to the test. Then, the crucible was placed in the oven for 10 min at 600^0C. Then it was cooled in room temperature and was weighted in a balance. The temperature was measured with a laser thermometer that is shown in the following picture.

Figure 31: Laser thermometer

Then, the specimens with the crucible were placed together on the oven at 600^0C until the resin was fully volatilized. The duration of each test was approximately 6 hours. In the next photo it is shown how does a specimen look like after the resin- burn off test.

Figure 32: Specimen after resin- burn off test

5.6.1 Optimal burn off time

To find the optimum time that is needed in order for the resin to be fully volatilized, a parametric study was conducted. In this study,12 specimens similar to those that were examined for the calculation of the density of the composite were used. Six of them were placed in the furnace at the same time and every 1 hour one of the specimens was removed. This test was repeated one more time. The specimens that were tested in the first test are shown in the following pictures.

Figure 33: Burned specimens (6000C) of the parametric study used to identify the optimal burn time

From the above illustrations, it is remarkable how the glass fibres have been wrinkled in the specimen that was burned for 7 hours. It seems like the weight of the fibres was affected after burning for so many hours. The optimum time was found to be 6 hours. In less than 6 hours the resin was not fully removed from the composite and the fibres were still unaffected from the high temperature. In the 2 specimens that were burned for 6 hours the resin was fully burned and at the same time the glass fibres were still intact.

5.7 Validation of the Void Content Measurement Method

For the following calculations 4 of the 9 specimens are presented in order to reduce the volume of numbers since the results were very close for all the 9 specimens. The remaining fibres were put on the scale and they were weighted. From the total initial weight of the specimen and the weight of the fibres, the weight of the resin for each specimen was calculated as follows:

$$W_{resin} = W_{total} - W_{fibrre}$$

In the table below, is shown the average values of the total weight and the weight of the resin and the fibres, as they were measured and calculated.

Number of Specimen	Total Weight (g)	Fibre Weight (g)	Resin Weight (g)
1	4.0709	3.04033	1.03057
2	4.45865	3.28449	1.17416
3	4.67458	3.47815	1.19643
4	3.83775	2.86026	0.97749

Figure 34: Measured weights

As mentioned, the Void Content was calculated based on the D2734. Now that the composite and the weight of the fibres and the resin are known, the void content can be calculated.

First of all, the **theoretical density** must be calculated as follows:

$$T_d = 100 / (R/D + r/d)$$

$$R\ (\%) = W_{resin/}\ W_{total}\ \text{and}$$

$$r\ (\%) = W_{fibres/}\ W_{total}$$

where:

T_d = the theoretical density,

R = the % of the weight of the resin in the composite

D = the density of the resin,

r = the % of the weight of the reinforcement in the composite, and

d = the density of the glass fibers.

In the following table the average values of the corresponding theoretical density for each specimen are illustrated, given that the density of the fibres and the resin are equal to d = 2.507 g/cm^3 and D = 1.6 g/cm^3, respectively. The values of the density of the fibres and the resin were given by the manufacturer.

An effort was made to verify those values. The value of the density of the fibres was calculated (2.507 gr/cm3) by measuring the weight of the fibres outside and inside the water and then following the same process as shown in the chapter 5.5.3.2. Calculating the density of the fibres was not possible due to 2 limitations. First of all, there was no access to bulk resin from the manufacturer. If there was access to bulk resin, then it would have been used to recreate the curing conditions so that resin in the same form with the composite would have been created and then measured. Due to the lack of bulk resin, a different method was

used. Peels of resin were removed from the top side of the specimens; however, their size was very small and they floated inside the water. Thus, it was not possible to measure their weight inside the water. Since the calculated density of the fibres (2.507 gr/cm^3) and the value given from the manufacturer (2.520 gr/cm^3) were identical, it was accepted that the value of the density of the resin (1.60 gr/cm^3) was correct too.

Number of Specimen	Theoretical Density (g/cm^3)
1	2.192378
2	2.181359
3	2.189351
4	2.190696

Figure 35: Theoretical Density

Finally, for the calculation of the void content, the following equation was used:

$$V = 100 * (T_d - M_d) / T_d$$

where:

V = void content (%) and

M_d = measured composite density

T_d = the theoretical density

Thus, the void content of the specimens was:

Number of Specimen	Measured Composite Density (g/cm^3)	Void Content (%)
1	1.933	11.83088

2	1.917	12.11902
3	1.935	11.61765
4	1.933	11.76319

Figure 36: Calculated void content

The pipe (from which the specimens were extracted) was given from the manufacturer with a void content of approximately 12% as it was measured from the manufacturer. The methods that were used were unknown. Both the method that the manufacturer used and the method conducted in this research shown almost the same results. The average void content from the 9 specimens was calculated 11.8895% while the manufacturer calculated it as approximately 12%. This fact strongly validates the effectiveness of the test method used in this research. So, the same test method was used to calculate the Low void content and the High void content specimens that were given by the manufacturer since the last did not measure the exact void content.

5.8 Void Content Measurement

Using the same method and calculations with the previous sub chapter the void content of the low velocity impacted specimens was calculated. As previously stated in the chapter 5.5.1 the void content cannot be calculated by extracting a specimen directly from the damaged area. Since the calculated void from the 4 corners of the impacted specimen were very similar, it was safe to assume that calculating the void content only from one of the four corners of the specimens was sufficient. The results are shown in the table below:

	10 Joule	20 Joule
Low Void Content	7.0216	7.1513
Low Void Content	6.8925	7.0551
Low Void Content	7.2162	6.9841
High Void Content	14.4520	14.3786
High Void Content	14.2585	14.4320
High Void Content	14.3952	14.4122

Figure 37: Void content of the impacted specimens

Having such precision in the calculations of the void content was not necessary, but it did not increase the time that the calculations needed, thus it was chosen to keep the calculations as detailed as possible in case that a new test would require such precision. Calculating the void content was necessary in order to assure that the specimens used in the impact tests were truly Low and High in void content.

6 Inspection of the Damaged Area

Closely Inspecting the damaged area was necessary in order to determine if linking was created between the voids due to the impact event. However. A difficulty is presented when trying to look inside the impacted area. By cutting the specimen in two pieces with a diamond cutter the impacted area was further damaged and examining it would create false observations.

Figure 38: Impacted specimen cut in the middle with a diamond cutter

A different technique was used. The specimen was cut with a diamond cutter but not in the middle. Instead the specimen was cut 5mm offset from the middle and then it was slowly trimmed down using grinding sheets. Initially it was grinded by hand with a P 400 grinding

sheet and then gradually reached to P 4000 grinding sheet until 5mm of material were removed. This process ensured that much less damage and alteration was forced in the damaged area.

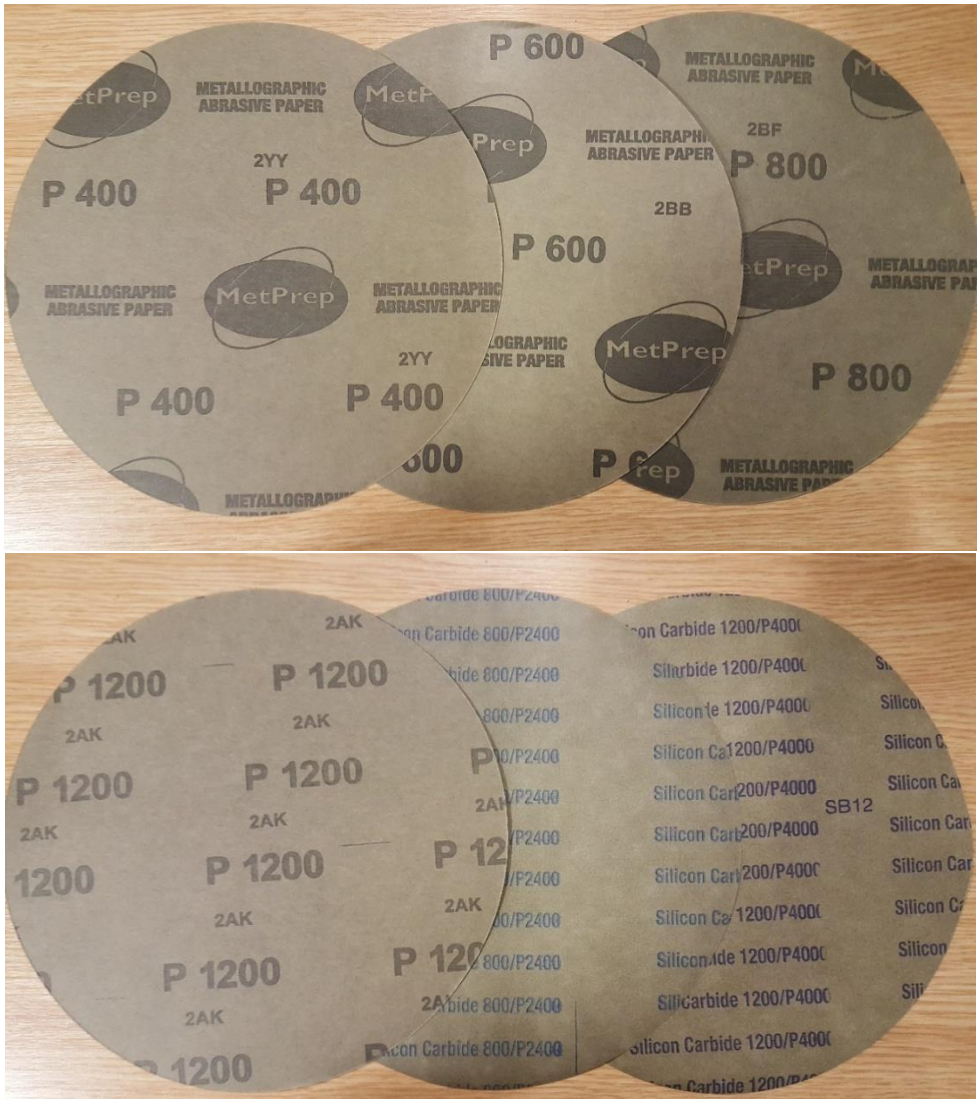

Figure 39: Grinding sheets (P400, P600, P800, P1200, P2400, P4000)

6.1 Camera

A regular consumer camera was used to closely inspect the damaged area after the grinding procedure. As shown in the pictures below the resolution and the zoom of the camera was

not sufficient and observations could not be made using them. Attention was given to the lighting which improved the results but not in an acceptable level.

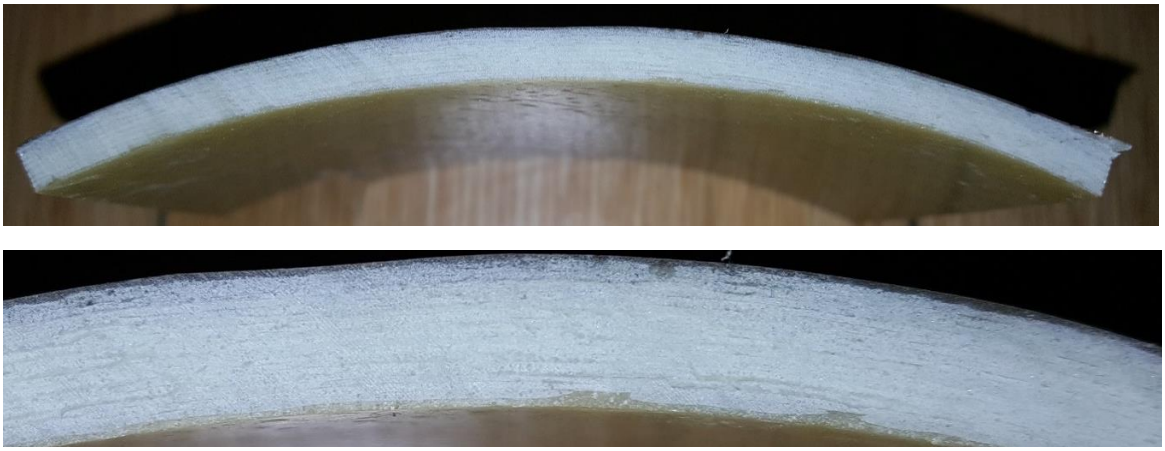

Figure 40: Photo of the impacted area using a regular camera

6.2 Advanced Camera

Since the previous equipment was not sufficient, a different method had to be used. The specimens were sent to an external researcher with access to a more advanced camera.

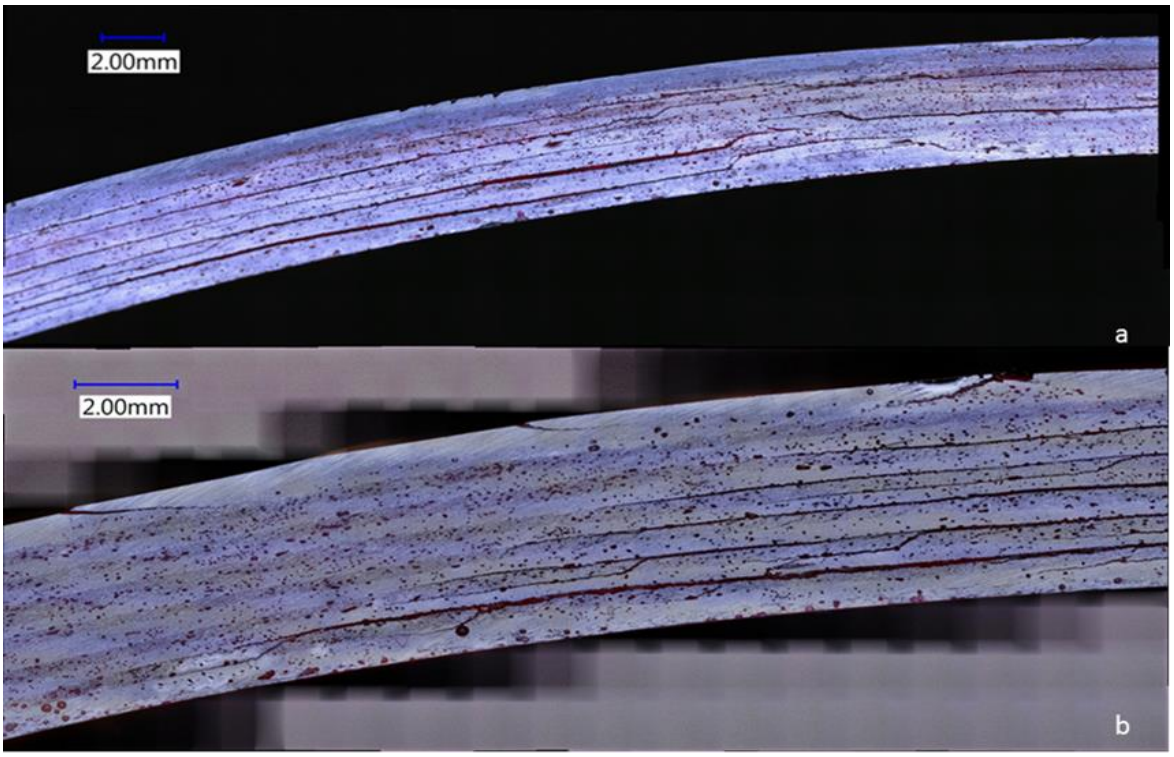

Figure 41: Photo of the impacted area using the advanced camera

The zoom and the quality of the images that were created were significantly superior compared to the previous equipment and made the observation process much easier.

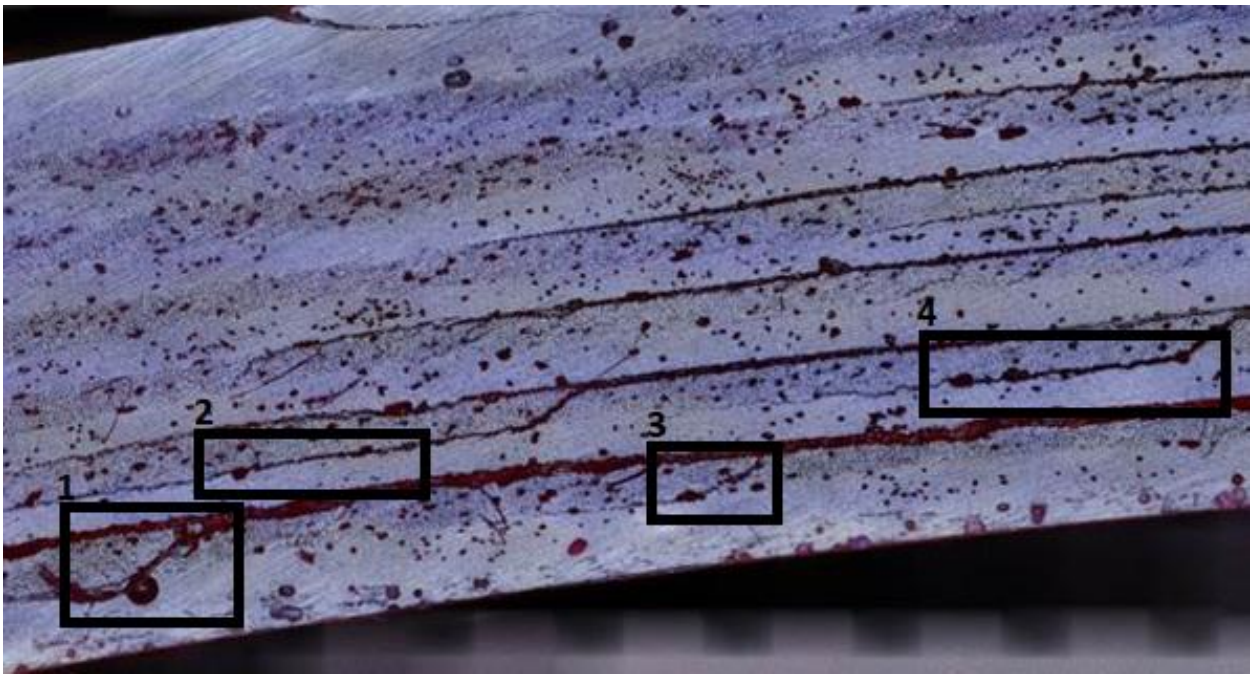

Figure 42: Close up photo of the impacted area using the advanced camera

Different types of damage can be observed in the impacted area. Between almost all the plies there is extensive delamination. Some of the cracks propagated from their ply to the next one. However, some cracks while leaving their initial ply they propagated in the interface between the plies. These specimens were impacted with 20J impact energy and their void content was approximately 6.5%.

The linking between the voids is very significant (1, 2, 3, 4). There was linking between the voids parallel to the interface (2,4). This type of linking can't create a path in order for the content of the pipe to leak. There was linking between the voids perpendicular to the interface of the plies (3,4). This type of linking can create a path in order for the content of the pipe to leak. However, this linking was extended between 2 plies only. It was estimated that the void content was between 3-

6.3 Conclusions

The linking between the voids after a low velocity impact event exists. For impact events up to 20 Joules the linking between the voids can extend up to 2 plies so there is no risk that the linking could extend from the top ply to the bottom ply through the thickness. For higher energy events this could be possible but further research must be conducted.

As it was shown in this chapter, the damage of the specimens was extensive, so a pipe made from the same materials would have similar behavior. Thus, a pipe made of glass fibres reinforced plastic that was impacted under low velocity with energy of 20 Joules should definitely be inspected so that its structural integrity could be evaluated.

7 Finite Element Analysis

The Finite Element method is a numerical method a computerized calculation method for the analysis of a structure. From the FEA a lot of data can be extracted, including the behaviour of a structure under specific conditions, the forces, stresses and displacements that are developed in any area of the structure, the failure mechanisms, etc. The financial impact of the introduction of the numerical models is great. The main reason that the FEA method has been developed is because a structure can be examined without the need of testing it or even manufacturing it. It can predict the response and the strength of a component, part or structure prior to its construction. One more advantage is that a structure can be tested without the need of testing machines. This is very important, especially, when a big structure like the fuselage or the wings of an airplane have to be tested.

On the other hand, the use of FEA requires very experienced engineers. Since it is a computer aided method, the results are extracted via complex equations. The edges of the elements are called nodes and the software develop equations for these nodes. Whatever happens inside the element is been neglected. The use of equation could content a lot of assumptions that could have as a result to overestimate the strength of the structure. For this reason, the FEA analysis must be very carefully carried out and the user must be able to identify through his or her experience and the current literature if the assumptions that have been done are correct. Thus, the FE analysis must always be followed by experiments that will be conducted in real conditions to avoid such mistakes.

There are a lot of available FE packages available in the industry, each of them has each limitations or advantages over the others. For example, Abaqus offers a very user- friendly environment, especially for the simulation of composite materials. In this study the Abaqus software will be opted for the analysis that will be conducted.

In finite element analysis the structure is being designed in the software and then it is discretized in very small parts. These parts are called elements. The software recognises only the regions, where there are elements and identifies the changes that are developed in each element separately. The greater number of elements, the higher precision of the analysis. The user inputs the data that will help the software to create the equations that are going to describe each element in each time period, which is called time increment.

To simulate a structure, there are some basic steps that must be followed. First of all, the geometry of the construction is introduced into a CAD program that is implemented into the FE software and the three-dimensional or two- dimensional model is been created. For more complex geometries, it is suggested to create the model in another CAD design and then import that design in Abaqus. For this project, the structure was designed in Abaqus. Initially, the impactor was designed as a rigid body that cannot be deformed and a reference point (RP) was defined as it is shown in the picture below. This point will allow the definition of the displacement or the load that the impactor will apply on the laminate. Then, the section of the pipe was designed.

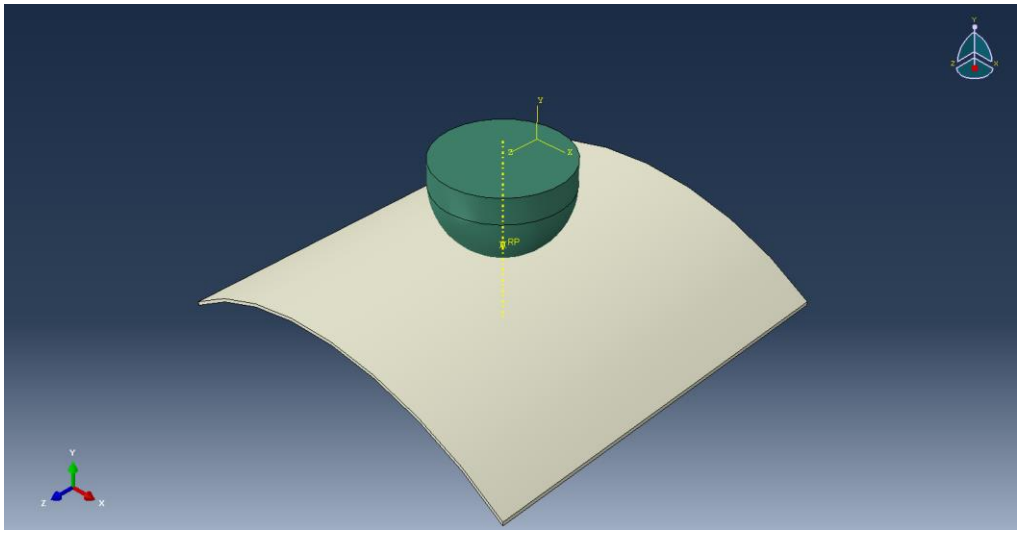

Figure 43: Illustration of the impactor and the laminate

The next step is to seed the structure, so that the number of the elements will be defined. It is important to add more elements in the areas that are more susceptible to break, there is bigger stress distribution or a significant change in the geometry. It is important also, to decide the type of the elements that are going to be used. For example, in geometries, where the thickness can be neglected, shell elements are recommended. Shell elements do not take into account the thickness of the structure and as a result the stresses in z- axis. They are the less precise but the most time efficient elements. Three- dimensional elements are opted for thicker structures. Their main disadvantage is that their response is more complex, thus they are time- consuming and sometimes the equations do not converge, and errors appears. One

of the solutions that seems to be promising in convergence issues, is to increase the number of the elements of change the convergence method that it is used. Abaqus, supports also the continuum shell elements that are going to be used in this study. They are applied in a 3D structure, like 3D solids and they have displacement degrees of freedom only, as well, whereas conventional shells have both translation and rotation degrees of freedom.

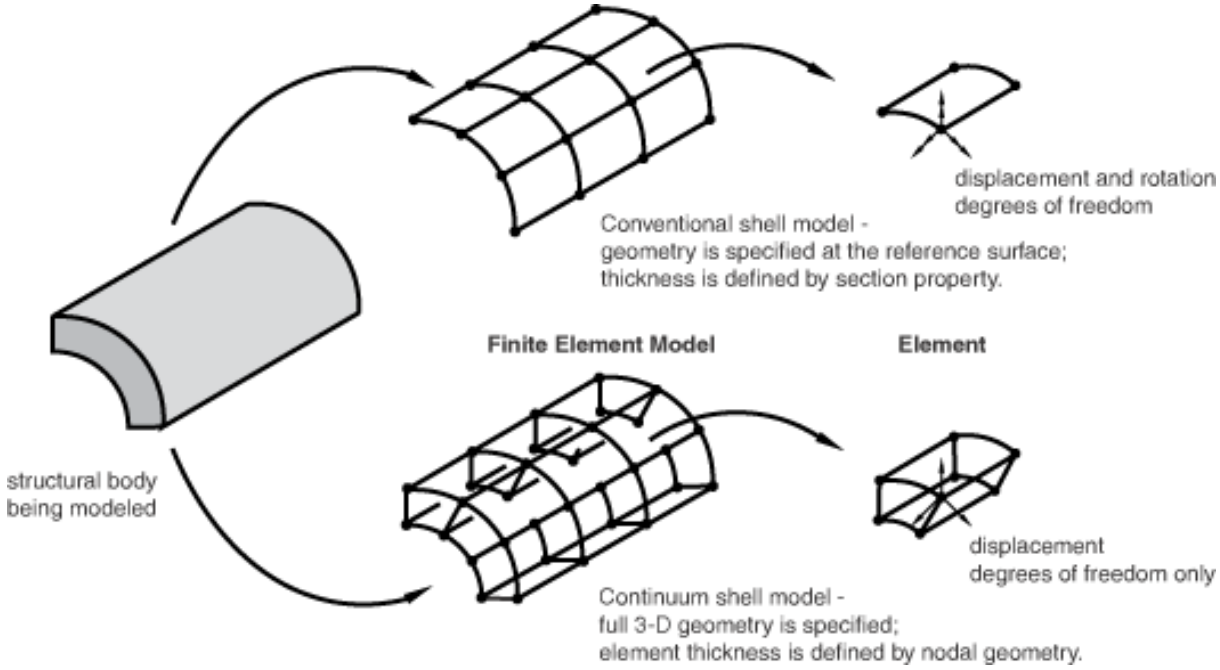

Figure 44: Continuum shell vs conventional shell elements (Source: 6.14 Abaqus Documentation)

One of the main challenges that was faced during the development of the models was the definition of the material. The pipes are GFRP manufactured with a method that is called filament winding. With this method it is difficult to determine the thickness of each layer and the number of the plies in order to insert them in the Abaqus software. Also, the manufacturer provides details only for the total properties of the pipe and not for the fibres, the resin or the ply, separately. So, the structure was modelled as a homogenous plate that was not made by composite material. Instead, it was assumed that the structure is been made by only one layer that has the equivalent properties that the manufacturer provides.

Figure 45: Filament winding (Source: i.ytimg.com)

After that, the structure was assembled and the impactor was located so that its RP would just come in touch with the laminate. Between the impactor and the laminate a tangential and normal interaction was set.

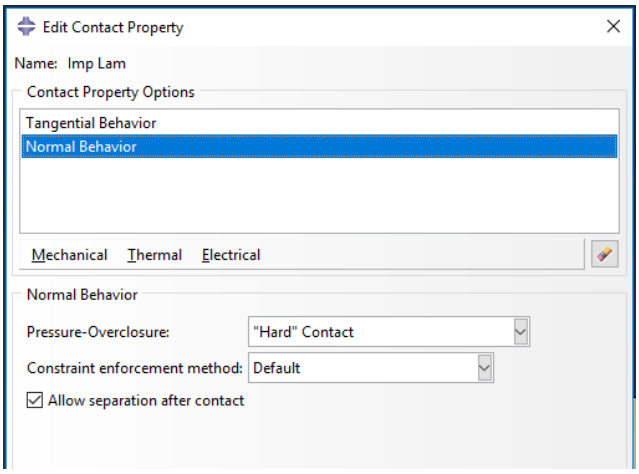

Figure 46: Interaction between the impactor and the laminate

The boundary conditions and the loading will be imposed in order for the experiments to more accurately be simulated. In the following picture it is shown how the boundary conditions were set and which surfaces were restricted.

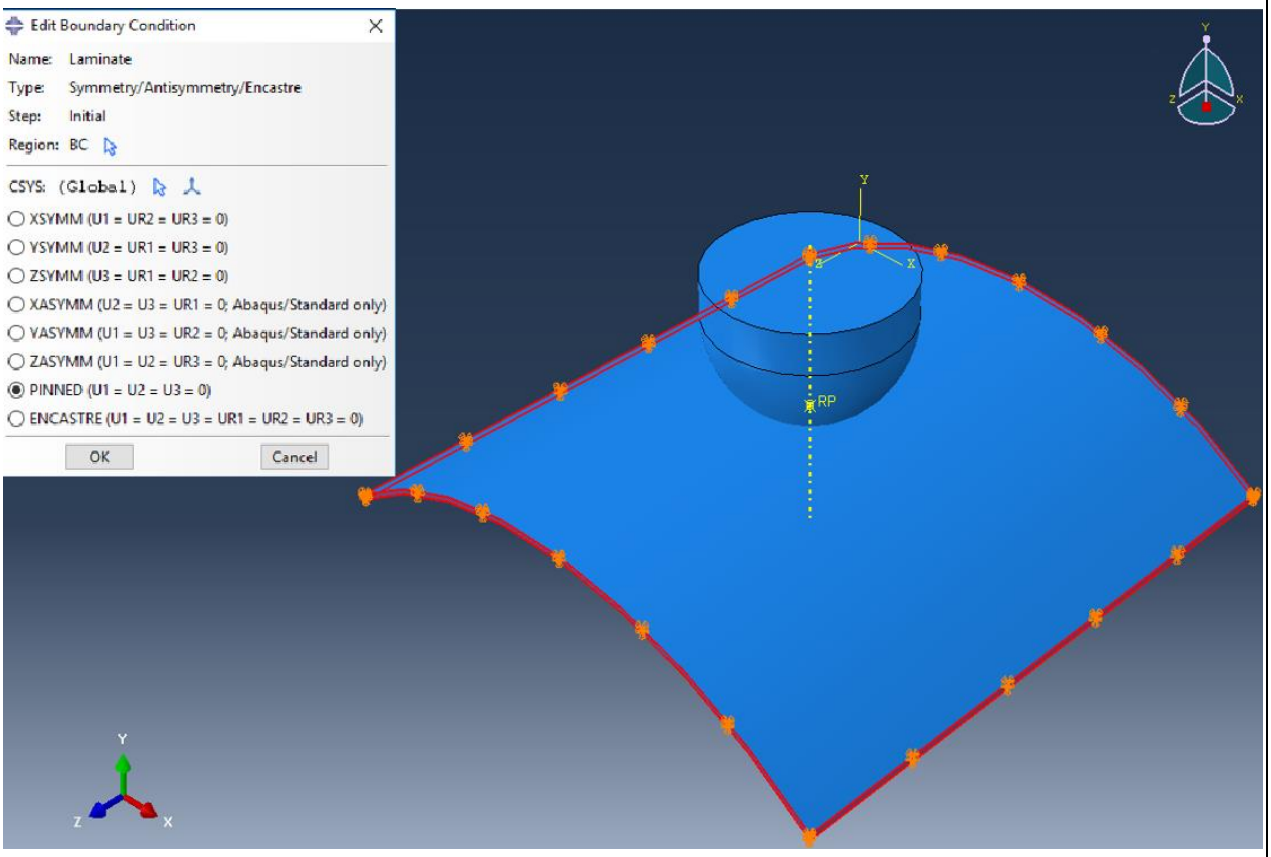

Figure 47: Boundary conditions

The impact loading could be simplified with the use of a static load. However, it would be very difficult to decide the correct value of the load. The most accurate approach is to design the impactor that was used in the experiments and apply on it the same value of the displacement that was measured during the test for each time increment.

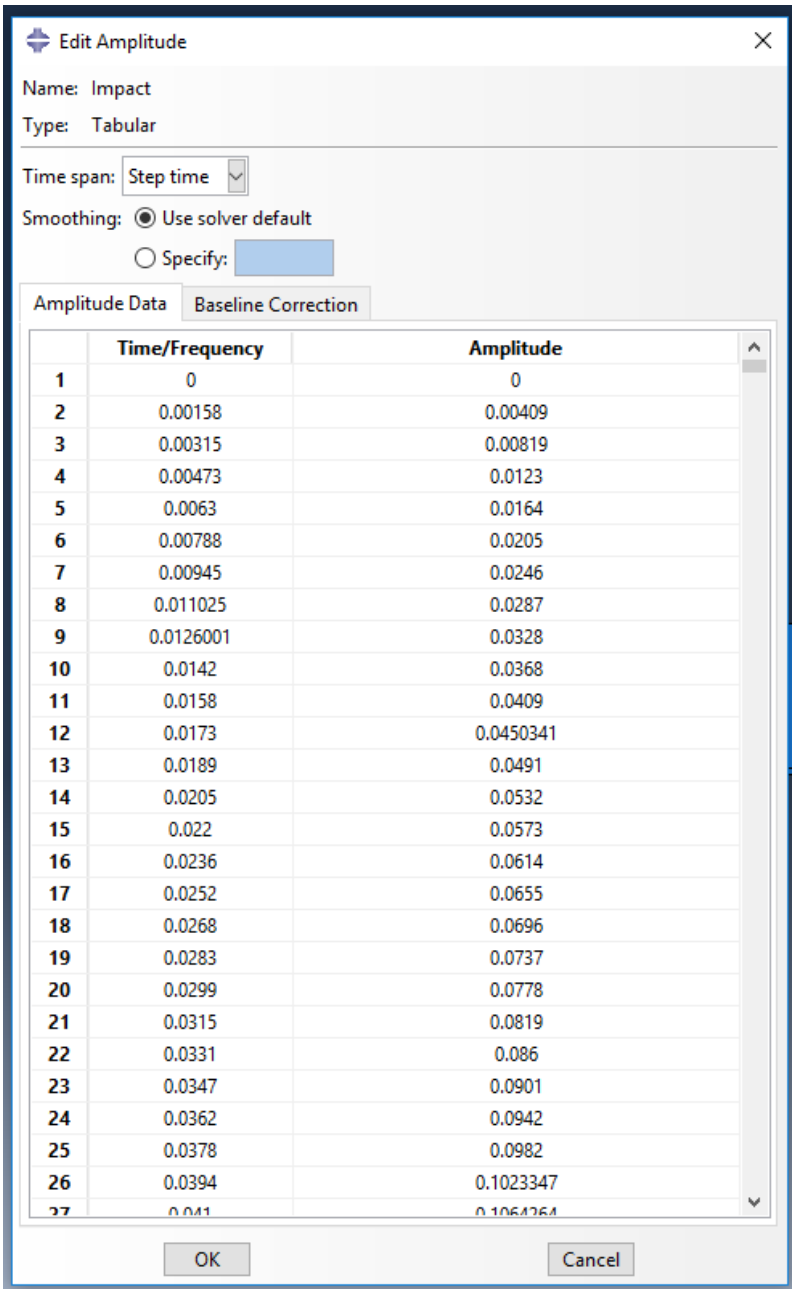

Figure 48: Amplitude / Time- Displacement

After the assembly of the structure and the definition of the step, the field and history outputs were set. The models were set to measure the stress distribution and the

displacements. This process is done with programs called pre-processor. When the data are resolved, they are entered into a program that will solve the problem. Such programs are called solver and use numerical methods for solving. Once the results have been resolved, a program called the post processor must be used to allow the designer to see the results.

Currently, there is no option for the simulation of the voids. One solution could be to randomly create pores in the structure. However, this solution is very random and time consuming. Simulating the voids content in a model is extremely difficult. A simple but efficient technique has been used. It has been proved that the properties of a structure are decreasing due to the existence of voids. (P. Olivier, 1995) So, based on the existing literature, the properties of the specimens will be reduced in order to simulate the voids content.

After the completion of the analysis, a comparison will be conducted between the experiments and the numerical models. The results are not expected to be exactly similar and leads in the necessity of further improvements in the numerical models. The main parameter that will affect the accuracy of the models is the assumption that the material is homogenous and because the shear stresses between the plies have not been taken into consideration. Increasing the number of the elements in the areas of interest is a first step to increase the accuracy but it is not enough to significantly increase the accuracy of the models.

In the following pictures, are shown the stress and displacement distribution for the laminate, whose void content was insignificant low. The stresses are measured in MPa and the displacements in mm.

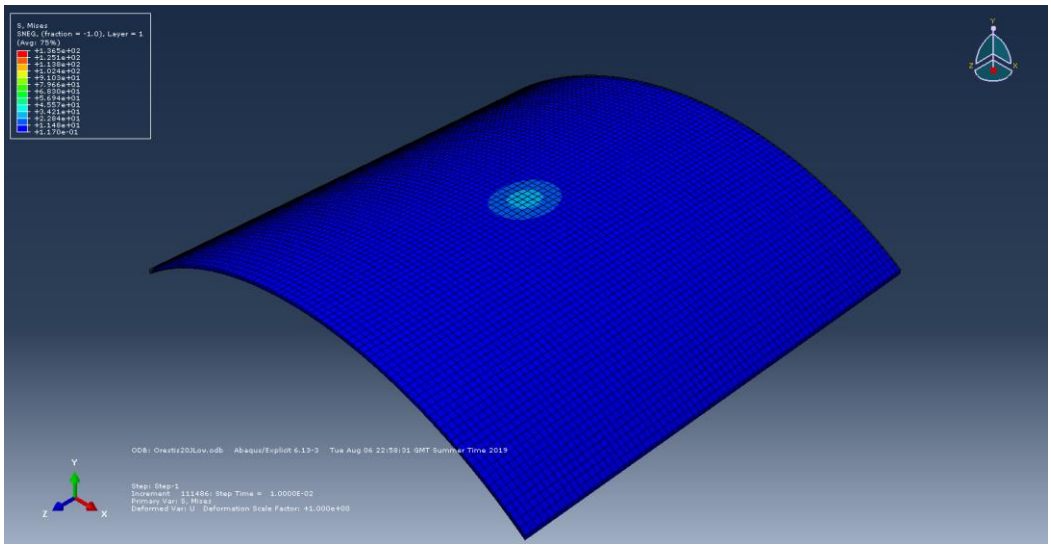

Figure 49 Stress distribution of the upper face based on Von Mises failure criterion

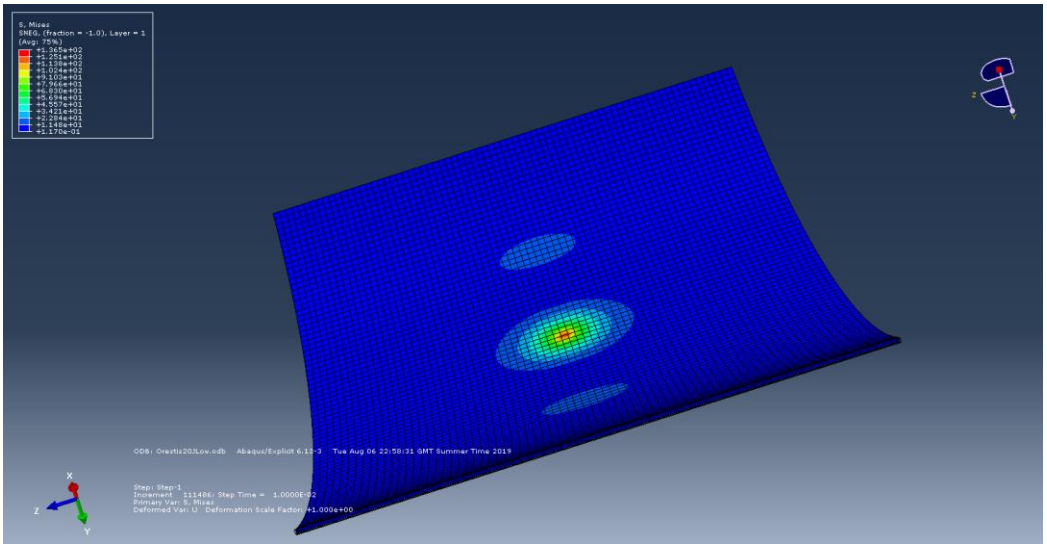

Figure 50: Stress distribution of the bottom face based on Von Mises criterion

The stresses are significant higher on the bottom face of the laminate. Based on the von Mises criterion, the maximum stress that has been developed on the structure is 136 MPa. The von Mises criterion calculates an average stress for every point that is given by the following equation:

$$\sigma_v = \sqrt{\frac{1}{2}[(\sigma_1 - \sigma_2)^2 + (\sigma_2 - \sigma_3)^2 + (\sigma_3 - \sigma_1)^2]}$$

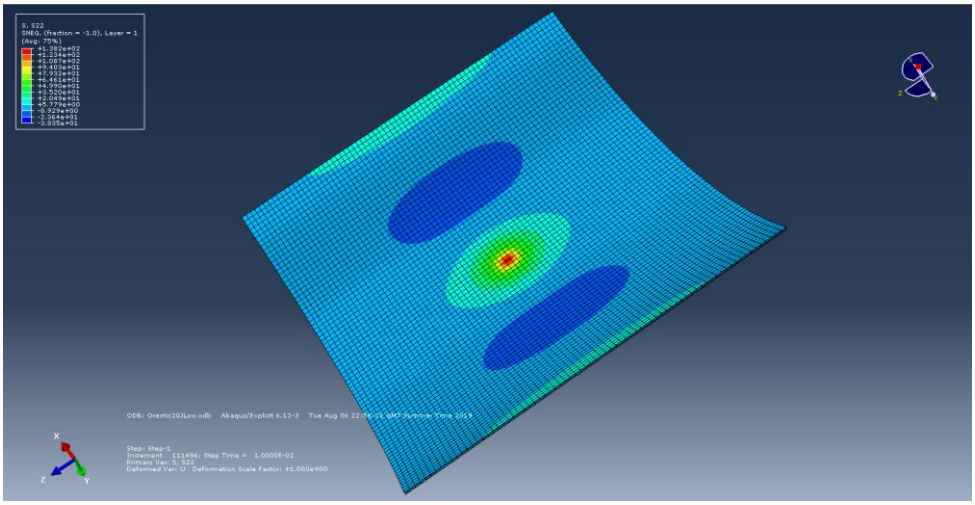

Figure 51: Stress distribution in the Y-axis

Only the stresses that are developed in the Y-axis have great interest, since their value is much higher in this direction which is similar to the direction of the impact loading. The maximum stress is 138 MPa and this value is similar with the maximum stress given by the Von Mises criterion.

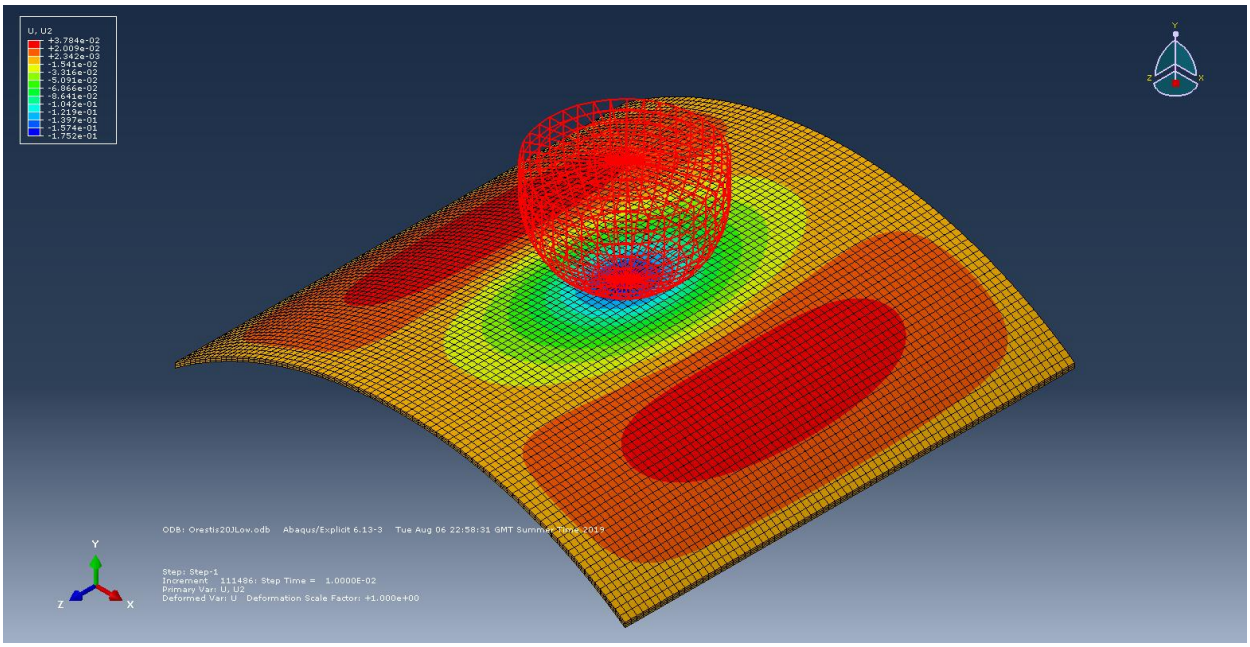

Figure 52: Displacement distribution in the Y-axis

The maximum displacement appears at the centre of the structure and has a value of -0.175mm. From the displacement distribution it can be observed that the displacements at the centre of the laminate are negative, which means that they follow the direction of the loading, whereas the displacements are becoming positive while heading on the edges of the laminate and they reach a maximum value of 0.038 mm.

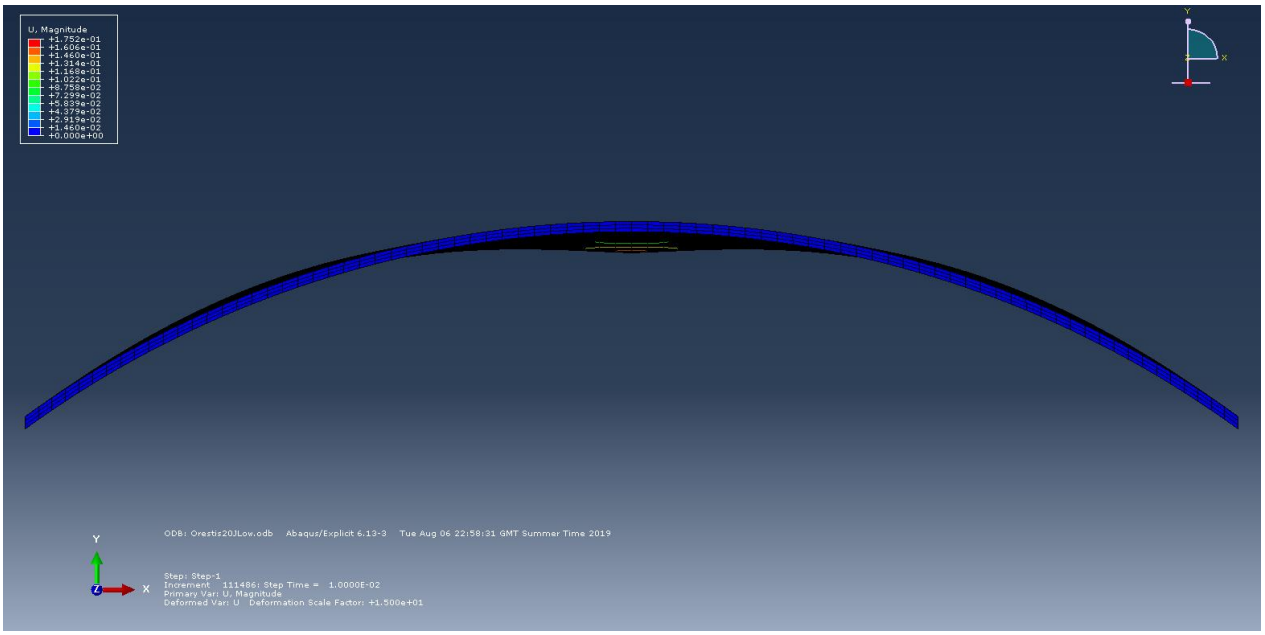

Figure 53: Illustration of the deformed laminate

The deformations have been magnified by 15, in order to visualize them. As it was anticipated, the deformations are mainly concentrated on the center of the laminate.

8. Conclusions

From the finite element analysis, the numerical results validated the experimental. The stress distribution and the displacements follow the actual geometry of the damage. The area where the impactor dropped, is the most highly stressed area. There, the maximum compression takes place, whereas the area close to the edges has been deformed in the opposite direction, due to tension.

The main problem that was faced during this Analysis was the fact that the glass fiber pipes that were simulated were made with a very common fabrication method for FRP pipes, filament wound. That problem was tackled, by **assuming that the structure is made of a homogenous material with orthotropic properties**. These properties have already been measured and provided by the manufacturer of the pipes. The problem with this is that the shear stresses between the plies that can cause delamination are not taken into account. However, the results correspond to the actual experimental response of the specimens.

The specimens that were tested under 20J impact energy presented similar behaviour independently of the void content. The specimens that were tested under 10J impact energy did not appear to have similar behaviour. From the results above the following can be concluded. When the impact energy is low the behaviour of the specimens cannot be predicted, and it is different every time. For higher impact energies the specimens behave in a more controlled way and therefore the curves were similar. By examining the high impact energy curves, it can be observed that **the void content did not appear to significantly affect the behaviour of the specimens**.

The linking between the voids after a low velocity impact event exists. For impact events up to 20 Joules the linking between the voids can extend up to 2 plies so there is no risk that the linking could extend from the top ply to the bottom ply through the thickness. For higher energy events this could be possible but further research must be conducted.

The damage of the specimens was extensive, so a pipe made from the same materials would have similar behavior. Thus, **a pipe made of glass fibre reinforced plastic that was impacted under low velocity with energy of 20 Joules should definitely be inspected afterwards** so that its structural integrity could be evaluated.

8.1 Future research

A study could be made in order to identify the most suitable boundary conditions for the model. The boundary conditions should give the ability to the laminate to behave as if it was part of the whole pipe. This could be achieved by modeling the whole pipe and examining the stresses on the area that the laminate was extracted. By examining the stresses on the modelled laminate itself and comparing them with the same area on the whole pipe the effectiveness of the boundary conditions could be evaluated. Changing the boundary conditions and repeating the comparing process would allow the researcher to identify more suitable boundary conditions.

An additional model could be made that would simulate a high void content laminate. The results could be compared with the low void content model and with the experiments that were conducted. It should be mentioned that the modelling process requires a lot of time since such a model requires approximately a day to run on an average workstation.

A more effective method could be used to examine the damaged area and identify the linking between the voids. Electron microscopy could provide a massively more detailed picture of the impacted area.

8 References

Bar-Cohen Y, C. R. L. (1982). Acoustic-Backscattering Imaging of Subcritical Flaws in Composites. *Mat. Eval.*, 970.

Bertović, M. (2016). Human Factors in Non-Destructive Testing (NDT): Risks and Challenges of Mechanised NDT. *Bundesanstalt für Materialforschung und -prüfung*.

Chamis, C., J. H. S. (1985). Impact resistance of fiber composites: energy absorbing mechanisms and environmental effects. *Recent Advances in Composites in the United States and Japan*, 325-345.

Cantwell, W. J. a. J. M. (1991). The impact resistance of composite materials — a review. *Composites, 22*(5), 347-362.

Charalambides, M., Kinloch, A. J., Wang, Y., & Williams, J. G. (1992). On the analysis of mixed-mode failure. *International Journal of Fracture, 54*(3), 269-291. doi:10.1007/bf00035361

Fransico C. (2015) Impact damage evaluation of Glass-Fiber Reinforced Polymer (GFRP) using the drop test rig - An experimental based approach, ARPN Journal of Engineering and Applied Sciences

Hagstrand, P.O., F. B., J.-A.E. Månson. (2005). The influence of void content on the structural flexural performance of unidirectional glass fibre reinforced polypropylene composites. *Composites Part A: Applied Science and Manufacturing, 36*(5), 704-715.

Hansong Huang, R. T. (2005). Effects of void geometry on elastic properties of unidirectional fiber reinforced composites. *Composites Science and Technology, 65*(13), 1964-1981.

Harris, B. (1980). Accumulation of damage and non-destructive testing of composite materials and structures. *Annales de Chimie-science de Materiaux*(5), 327-339.

James, C. (1995). Co-mingled thermoplastic prepregs industrial applications. In: Proceedings of ICCM-10. *Whistler Canada*, 757–764.

Jeong H., D. K. H. (1995). Experimental analysis of porosity-induced ultrasonic attenuation and velocity change in carbon composites. *Ultrasonics, 33*(4), 195-203.

Lin Ye, K. F. (1993). Mode I interlaminar fracture of co-mingled yarn based glass/polypropylene composites. *Composites Science and Technology,, 46*(2), 187-198.

Manson, J.-A.E. , M. D. W., N. Bernet. (2000). Composite Processing and Manufacturing—An Overview. Pergamon. *Pergamon*(577-607).

Ozden O. Ochoa, M. M. S. (2005). Offshore composites: Transition barriers to an enabling technology. *Composites Science and Technology, 65*(15-16), 2588-2596.

P. Olivier, J. P. C., B. Ferret. (1995). Effects of cure cycle pressure and voids on some mechanical properties of carbon/epoxy laminates. *Composites, 26*(7), 509-515.

Richardson, M.O.W., M. J. W. (1996). Review of low-velocity impact properties of composite materials. *Composites Part A: Applied Science and Manufacturing, 27*(12), 1123-113

Salama MM, M. E., Spencer B, Hanna S, Hsu TM, Stjern G. (2001). Composite risers are ready for field applications – status of technology, field demonstration and life cycle economics. *Proceedings of 13th annual deep offshore technology conference*.

Salkind, M. J. (1976). Early Detection of Fatigue Damage in Composite Mtaerials. *JA Aicraft, 13*.

Standard Practice for Conditioning Plastics for Testing. *D618 − 13*.

Scott, I.G., C. M. S. (1982). A review of non-destructive testing of composite materials. *NDT International, 15*(2), 75-86.

Vary A., K. J. B. (1977). Ultrasonic evaluation of the strength of unidirectional graphite-polyimide composites. *NASA Technical Reports*.

8.1 Standards

ASTM D618 - 13 Standard Practice for Conditioning Plastics for Testing

ASTM D772 - 18 Standard Test Method for Evaluating Degree of Flaking (Scaling) of Exterior Paints

ASTM D2734 - 16 Standard Test Methods for Void Content of Reinforced Plastics

ASTM D4000 - 16 Standard Classification System for Specifying Plastic Materials

ASTM D7136 / D7136M - 15 Standard Test Method for Measuring the Damage Resistance of a Fiber-Reinforced Polymer Matrix Composite to a Drop-Weight Impact Event